RANDOM FIELD MODELLING OF RAINFALL INDUCED SOIL MOVEMENT

Martec Report No.: TR-01-02

D. Brennan
U. Akpan
I. Konuk
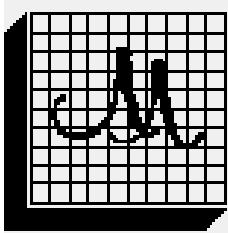A Zebrowski

Canada

Natural Resources Canada

Ressources naturelles Canada

Prepared for:

Geological Survey of Canada
Terrain Sciences Division
601 Booth Street
Ottawa, ON, K1A 0E8

Contract No.: 23397-9-S054/001/SS
SSC File No.: O32SS-23397-9-S054

Martec Limited
Advanced Engineering and Research Consultants

400-1888 Brunswick Street   101-717 boul St. Joseph
Halifax, NS, B3J 3J8   Hull, PQ, J8Y 4B6
Tel: (902) 425-5101   Tel: (819) 595-3526
Fax: (902) 421-1923   Fax: (819) 595-1739

February 2001

ABSTRACT

The development and incorporation of the latest enhancements to the PRESAP analysis codes are described. This work includes the development of specialized probabilistic methods designed to model precipitation induced slow slope movement using random field modelling techniques.

This report is comprised of eight chapters. The first five provide background information dealing with the scope/motivation for this project, a review of the work conducted during the previous phase of the PRESAP project, plus a series of literature reviews which considered the issues related to random field modelling of soil properties, rainfall, and stochastic finite element methods. In chapter six, a description of the random field modelling strategy developed for this project is provided. In chapter seven, details related to the software implementation of the modelling strategy are presented. In chapter eight, the results from a series of rain induced slope movement computer simulations are provided. The report concludes with chapter nine, which provides a summary of the work conducted under this research project and a series of recommendations for future work.

ACKNOWLEDGEMENTS

GLOSSARY OF TERMS

Auto-correlation Function
A function that measures the degree of similarity between values of a random field at different locations. Example slope movements at different locations.

Bayes Theorem
A theorem concerning conditional probabilities of the form $P(A \mid B) * P(B) = P(B \mid A) * P(A)$, where *P(B)* and *P(A)* are the unconditional (or a priori) probabilities of *B* and *A*, respectively.

BLUE
Best linear unbiased estimator is a technique for estimating the statistically properties of random fields or random variables.

Correlation
This is the measure of the degree of similarity between two random variables. When the two random variables that are being compared are the same, for example slope movement at two separate locations, the correlation is said to be an auto-correlation. When the two random variables represent different properties (i.e.: rainfall and slope movement) the correlation is said to be cross-correlation.

Correlation Structure
A function used to represent the correlation between any two locations in a random field.

Distribution
A distribution of measures or observations is the frequency of these measurements shown as a function of one or more variables, usually in the form of a histogram. Experimental distributions can thus be compared to theoretical probability density functions.

Distribution Function
The term distribution function is short for cumulative distribution function and describes the integral of the probability density function: a random variable X has the (cumulative) distribution function F(X), if the probability for an experiment to yield an X < x is

$$F(x) = P(X < x) = \int_{-\infty}^{x} f(\xi)d\xi$$

Histogram
Measured or generated data can be grouped into bins, i.e.: discretized by classifying into groups each characterized by a range of values in characteristic variables. The resulting graphical representation, usually limited to one or two variables, is called a histogram.

Homogeneous Random Field.
A random field is considered homogeneous when its mean value and variance do not depend on the location and its correlation is dependent solely on the distance between the variables.

IMSL
The IMSL math library is a collection of FORTRAN routines and functions useful in research and

mathematical analysis.

Multi Component Partitioning
A technique for transforming a non-homogeneous random field into a series of homogeneous random fields.

Non-Homogeneous Random Field
A random field whose statistical properties are a function of location.

Phenomenological Model
A perceived cause is (i.e.: rainfall) is mathematically linked to an effect (i.e.: ground movement) without attempting to model the mechanics of the relationship.

Probability Density Function
If a random variable X has a cumulative distribution function $F(x)$ which is differentiable, the probability density function is defined as $f(x) = \dfrac{dF(x)}{dx}$. The probability of observing X in the interval $x \leq X < x + dx$ is then $f(x)dx$. For a collection of several random variables, $X_1, X_2, ..., X_n$ the joint probability density function is $f(x_1, x_2, ..., x_n) = \dfrac{\partial^n F(x_1, x_2, ..., x_n)}{\partial x_1 \partial x_2 ... \partial x_n}$

Random Variable
A real random variable $X(\omega), \omega \in \Omega$, is a set function defined on Ω such that for every real number x, there exists the probability $P(\omega : X(\omega) \leq x)$. In other words, the real function $X(\omega)$ maps a sample space Ω into the real line R. In this definition, x represents the range of values that the random variable X can take.

Random Field
A random field can be defined as a family of spatially correlated random variables or random processes.

Examples of random fields are rainfall, soil properties and slope movement.

Sampling from a Probability Density Function
Frequently, a random sample is required that exhibits a known probability density function. Random number generators, on the other hand, usually supply samples with a uniform distribution, typically between 0 and 1. What is needed is a means for converting the uniform probability density function. If the a random number generator supplies the value r, the variable x is obtained by solving $\int_{-\infty}^{x} f(x)dx = r$ for x.

Slope Creep
Slow slope movement. Typically smaller than 100 mm per year.

Stochastic Finite Elements
A collection of techniques for incorporating random variables or fields into traditional finite element numerical methods.

Variance
This is the square of the standard deviation of a random variable.

White Noise Process
In the frequency domain, white noise is defined by a spectral density function that is constant for all frequencies. This property of white noise implies that the process is completely uncorrelated with itself at all time lags expect zero. Hence, the process is "noise", i.e.: completely incoherent.

NOTATION

$\hat{r}\,(x(t), y(t), z(t))$ represents a spatial location.

$\omega(\hat{r})$ represents a realization or sample of a random field at location $\hat{r}$.

$\mu(\hat{r})$ represents the mean value of a random field at location $\hat{r}$.

$\tau(\hat{r})$ represents the trend component of a random field (or mean value) at $\hat{r}$

$\sigma^2(\hat{r})$ represents the variance of a random field at location $\hat{r}$.

$f(\hat{r})$ represents the zero trend fluctuating component of a random field at location $\hat{r}$

$\text{cov}(\omega(\hat{r}))\omega(\hat{r}^1)$ represents the autocovariance function of a random field at two locations $\hat{r}$ and $\hat{r}^{1.}$

$\rho(\hat{r}, \hat{r}^1)$ represents the autocorrelation function of a random field at two locations $\hat{r}$ and $\hat{r}^{1.}$

δ represents the scale of fluctuation of the correlation function.

$\hat{c}[d]$ represents the moment estimator of the autocovariance function of a homogeneous random field estimated for a separation distance d.

θ represents a vector of parameters used to define the autocovarince function

$f(x)$ represents the probability density function for the random variable x.

$L(x_1, x_2, ..., x_n)$ represents the joint likelihood function of the collection of random variables $(x_1, x_2, ..., x_n)$.

K represents the global finite element stiffness matrix.

U represents the vector of nodal displacement.

F represents the global nodal load vector.

β represents the reliability index.

$g(X)$ represents a limit state function (a function of a series of random variables X).

t represents time.

P_f represents the probability of failure for a system.

$p_{\underline{x}}$ represents the joint probability density function of several random variables.

TABLE OF CONTENTS

LIST OF TABLES

LIST OF FIGURES

1.   INTRODUCTION

Scientists have been able to reach some important conclusions about climate change:

- the basis for concern is scientifically sound;

- human influence on climate appears to be discernible;

- the risks of danger are real and significant;

- the magnitude and distribution of regional danger is not as certain as we would like;

- the greatest danger may be associated with a change in the frequency and severity of extreme weather events; and

- the rationale for action is clear

While the exact rate and magnitude of regional climate changes are not yet known, precautionary action to reduce the risks, both through reductions in emissions of greenhouse gases and adoption of measures to adapt to changes in climate appears to be justified (McBean and Everall – 1998).

1.1   Climate Change Action Fund

In February 1998, the federal government established the Climate Change Secretariat. The Secretariat has three main objectives:

1) Serving as a focal point for the development of the federal government's domestic policy and programming on climate change;

2) Coordinating, in cooperation with provincial officials, the development of a National Implementation Strategy to meet the greenhouse gas emission reduction targets established in the Kyoto Protocol (aka the "National Climate Change Process"); and

3) Managing the Climate Change Action Fund.

The Climate Change Action Fund (CCAF) was established in order to build a policy foundation and to initiate early action to address climate change. While the majority of the Action Fund will address the reduction of emissions of greenhouse gases to meet the targets set out under the Kyoto Protocol, a portion of the funding has been set aside for work on climate science, impacts and adaptation.

1.2 Adaptation Strategies for Oil and Gas Infrastructure

The "Adaptation" component of the Action Fund will focus on developing a suitable and accessible knowledge base for wise and prudent decision making through investment in detailed research, consultations and case studies. This body of knowledge will enable researchers to better understand the need for greenhouse gas reductions and to identify and implement the most appropriate portfolio of response strategies to reduce the negative impacts of climate change and take advantage of the positive ones.

Adaptation strategies for oil and gas infrastructure clearly fall within the scope of the Action Fund. The threats posed by climate change to Canadian oil and gas infrastructure are many and varied, with significant environmental, social, and economic implications. In a recent study conducted by the Geological Survey of Canada (http://sts.gsc.nrcan.gc.ca/permafrost/), it was found that over half of the discontinuous permafrost zone in the Canadian Arctic would disappear as a result of a warming of 4 to 5 degrees, and the boundary between continuous and discontinuous permafrost would shift northward by hundreds of kilometers. In addition, climate change could potentially lead to a more vigorous hydrological cycle. As a result, Canada can expect an increase in flooding events due to more intense rainfall and snowfall in some regions, while drought events will rise as the number of dry days increases in other areas.

1.3 Rainfall Induced Slope Movement

In addition to the risks posed above, the projected changes in precipitation are also expected

to increase the potential for ground movement and slope instability. One of the primary causes of slow ground movement is the duration, amount and intensity of rainfall (Konuk, 1998). It is well known (McCarthy (1998)) that the infiltration of rainwater into soil increases the soil weight, slope load and pore water pressure. These changes in soil properties may result in a decrease in the soil shear strength, and as a result, may lead to an increase in the likelihood of soil movement. Consequently, this soil movement induces additional loads on neighboring structure (such as pipelines), resulting in increased strain levels that pose a risk to the integrity of these structures. In addition, existing assessment criteria, which are largely based on empirical or semi-empirical methods, do not account for the spatial variability of soil properties and are designed to utilize instantaneous (fixed) values of important material parameters without providing guidelines for making estimates of their impact on future pipeline reliability. Furthermore, most of the existing empirical/semi-empirical methods do not have a framework for modelling complicated loading and boundary conditions.

1.4   Random Field Modelling

In order to assess the effect of rainfall-induced ground movement on the structural integrity of pipelines, a rational and systematic procedure that fully accounts for all the spatial and temporal variabilities inherent in the rainfall, the soil, the pipeline, and the interactions between these parameters must be developed. Such a modelling capability can be provided by adopting a random field based probabilistic modelling and analysis strategy (Vanmarcke (1983) and Orisamolu, et al. (1999)).

In a previous study, sponsored in part by the Geological Survey of Canada, researchers at Martec Limited successfully developed a random field based probabilistic modelling software tool for use in the assessment of the structural reliability of damaged pipelines (PRESAP – Orisamolu, et. al. (1999)). This work demonstrated that the random field modelling approach is ideally suited for the representation of complex spatial random phenomena such as rainfall and slope movement. Random fields offer an important

mathematical framework via which a meaningful representation of parameters defined over a given domain can be modeled. In particular, a random field approach can efficiently account for different severity and variability levels for soil properties and rainfall intensity in the spatial domain via partitioning of a non-homogeneous random field representation into multiple homogeneous segments (each segment having a distinct correlation structure and set of statistical parameters). Furthermore, the correlation structure, which is derived during the random field characterization, can be used to measure the degree of similarity in behavior (or properties) associated with any two points in the field, and as a result, can reveal the heterogeneities and the anisotropy that may be present.

1.5 Modelling Rainfall Induced Soil Movement Using PRESAP

This current project has been proposed in order to extend the modelling capabilities of the PRESAP software tool to include slope instability (ground motion) damage models. The motivation behind this endeavor stems from the fact that a considerable number of pipeline networks are located in areas where potential ground movements pose a real and significant threat to structural integrity. The objectives and goals of this scientific effort will be to provide industry and regulators with a software tool capable of:

- Modelling the relationship between rainfall and slope movement for particular pipeline routes;
- Predicting the likelihood of exceeding thresholds for slope movement for various levels/intensity of precipitation, and;
- Providing risk maps for slope movement which can be used as an aid in pipeline route selection and adaptation strategies for the design and maintenance of oil and gas infrastructure;

The main source of data to be used to characterize the slope movement random fields will be supplied by the Scientific Authority and is in the form of monthly time histories. Data related to the mechanical properties of the soil will not be available. As a result, a

phenomenological modelling approach will be used to establish the relationship between precipitation and ground movement. Phenomenological models, which have been used in similar applications, relate a perceived cause (i.e.: precipitation) to an effect (i.e.: ground movement) without attempting to model the mechanics of the relationship. This type of approach allows for the prediction of soil movement based solely on rainfall or snowfall.

1.6 Organization of Report

This report is comprised of eight chapters. The first five provide background information dealing with the scope/motivation for this project, a review of the work conducted during the previous phase of the PRESAP project, plus a series of literature reviews which considered issues related to random field modelling of soil properties, rainfall, and stochastic finite element methods. In chapter six, a description of the random field modelling strategy developed for this project is provided. In chapter seven, details related to the software implementation of the modelling strategy are presented. In chapter eight, the results from a series of rain induced slope movement computer simulations are provided. The report concludes with chapter nine, which provides a summary of the work conducted under this research project and a series of recommendations for future work.

2.   PRESAP PHASE I REVIEW

Support for the development of the PRESAP project was motivated by an interest in adopting new methodologies for assessing the impact of corrosion damage on the structural integrity of pipelines. Prior to the initiation of PRESAP, corrosion defect assessment criteria, such as those embedded in the CSA codes, were largely based on overly conservative empirical or semi-empirical methods. In contrast, PRESAP offered a probabilistic mechanics based approach for performing residual strength assessment on damaged (or degraded) pipelines. By adopting a probabilistic based approach, PRESAP provided a number of clear advantages over other more conventional techniques.

- A probabilistic approach is capable of rationally accounting for the various uncertainties that affect structural integrity;
- Probabilistic modelling allows user's to perform sensitivity analysis (sensitivity information can be used to identify the most important parameters that effect residual strength);
- The probabilistic approach provides a unique framework for considering the interaction of multiple failure modes via stochastic system models, as well as the modelling of the same failure mode for several pipeline segments.

2.1   Key Elements of the PRESAP System

The methodology and supporting software developed during the initial phase of the PRESAP project was comprised of four key elements (see Figures 2.1 and 2.2):

1. Database management (collection and storage of corrosion pit data);
2. Random variable/random field characterization (i.e.: representation of corrosion as individual random variables or collections of random variables within a random field);
3. Model/System definition (definition of limit state functions used to estimate the probability of failure);
4. Reliability assessment algorithms (used to compute probability of failure, sensitivity information, etc.)

2.2　　Limit State Functions

For readers unfamiliar with the use of limit state functions, consider the case of a structure having a load carrying capacity (or strength) defined by the function $R(u_1,u_2,...,u_n)$, where $u_1,u_2,...u_n$ represent the random variables (or random fields) which influence the structural load carrying capacity. In addition, consider the variable $S(v_1,v_2,...,v_3)$ that is defined by the random variables $v_1,v_2,...,v_3$ and acts as a load on the structure. Using these definitions for load and resistance, it is then possible to define an operational margin of safety for the structure in terms of a limit state function Z,

$$Margin\ of\ Safety = Z = R(u_1,u_2,...,u_n) - S(v_1,v_2,...,v_3) \tag{2.1}$$

Figure 2.3 provides a graphical representation of the limit state function using the probability density functions for load and strength (p_S and p_R respectively). When R = S (or Z = 0), the structure reaches the limit state as defined by Z. In this case the probability of failure (P_f) is represented by the shaded volume of the joint probability density function ($p_{\underline{x}}$). Mathematically this volume can be calculated using the formula provided in Equation 2.2,

$$P_f = P(Z < 0) = \iint_{Z(x)<0} ... \int p_{\underline{x}}(x)dx_1...dx_m \tag{2.2}$$

where $x_1,x_2,...,x_m$ represent all the parameters used to define the load and resistance for the system. Note that every parameter has its own probability density function, and as a result, the evaluation of the probability of failure using Equation 2.2 (i.e. a level III approach) can lead to very complex and computationally intensive calculations. In addition, finding reliable probability density functions for all random variables involved is also a difficult and time-consuming process. For situations where direct integration of the joint probability density function is not possible, a number of approximate methods are available:

1. Level II: P_f is represented by means of simplified functions;

2. Level I: For every parameter involved in the definition of the load or resistance, a partial safety factor is used;

3. Level 0 (deterministic approach): Some maximum load and minimum strength is established on the basis of experience and/or intuition and one overall safety factor is applied. This is clearly not a probabilistic approach at all.

As an example of how limit state functions can be used in practice, consider an analysis involving the cantilevered beam represented in Figure 2.4. For the purposes of this example, we wish to compute the likelihood that the tip deflection (u) will exceed 1.92 cm. As a result, the appropriate limit state function is provided below in Equation 2.3.

$$Z = R - u = 1.92 - u(w, E, I, L) = 1.92 - \frac{wL^4}{8EI} \tag{2.3}$$

See Table 2.1 for a list and description of the random variables w, E, I, and L.

Table 2.1: Cantilevered Beam Variable Definition

Variable Symbol	Description	Distribution	Mean Value	Standard Deviation
w	Uniform Load	Normal	0.08	0.016
E	Young's Modulus	Normal	29000	1740
I	Moment of Inertia	Normal	301	15.05
L	Length of Beam	Fixed	192	N/A

In this case, since we are dealing with only a relatively small number of random variables, Monte Carlo simulation can be used to indirectly solve for the probability failure, thus avoiding the direct integration of the joint probability failure. The basis of this method is quite simple. For all the random variables involved in the definition of the limit state function (i.e.: w, E, I, and L) a value is generated at random, taking into account the particular probability density function of that variable. Once values for all the variables have been established, the resulting value for Z is computed using Equation (2.3). This procedure is repeated N times, after which P_f is defined as

$N_F\big/N$ (where N_F represents the number of times Z < 0). For the case of the cantilever beam, the Monte Carlo estimate for the probability of failure is 14.7%.

2.2.1 Series and Parallel Limit State Functions

In many applications the limit state of structure cannot be defined in terms of a single function. In such cases, it is more appropriate to define failure in terms of a combination of limit state functions, which together can be modelled as series and/or parallel systems (each individual limit state function is modelled as "component" in the system). If a series system analogy is adopted, then failure of any single component will result in the failure of the system as a whole. In a parallel system, however, all components must fail before the system itself reaches failure.
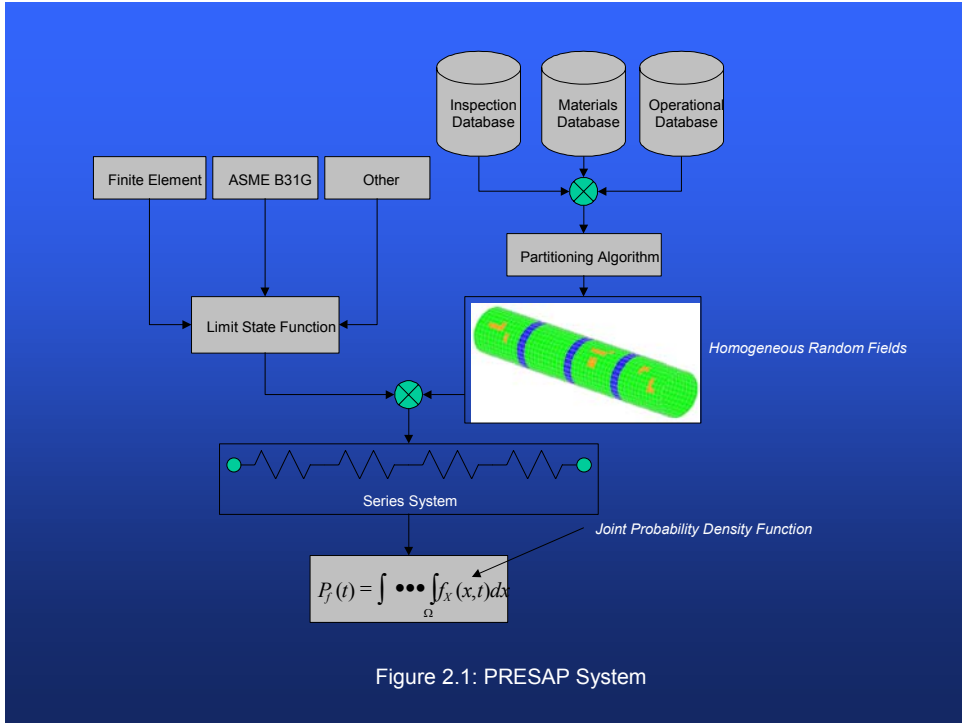
Figure 2.1: PRESAP System
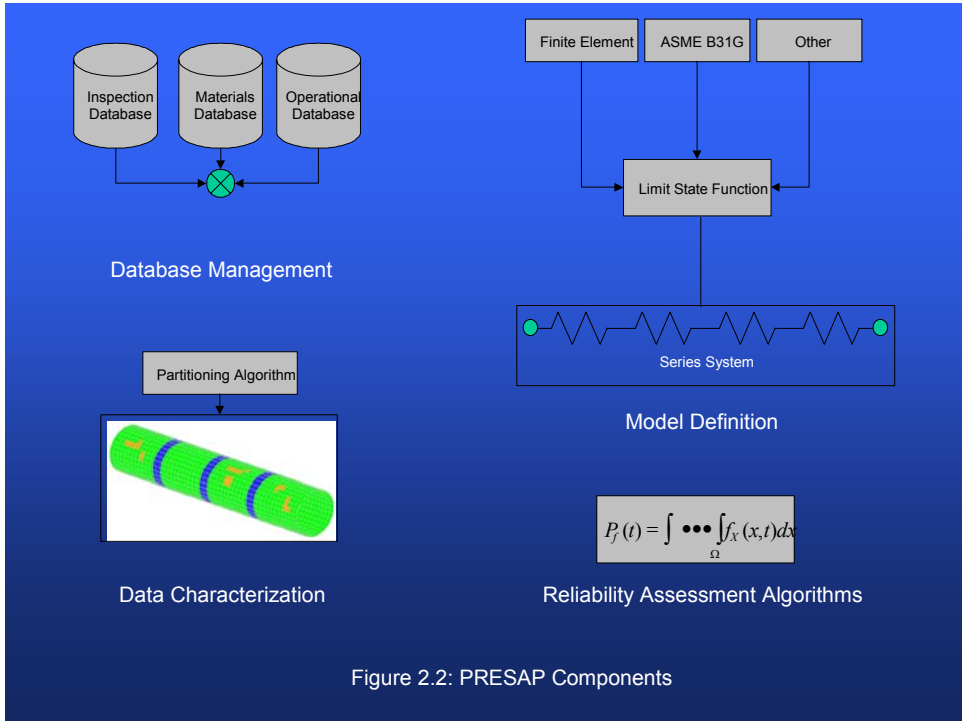
Figure 2.2: PRESAP Components
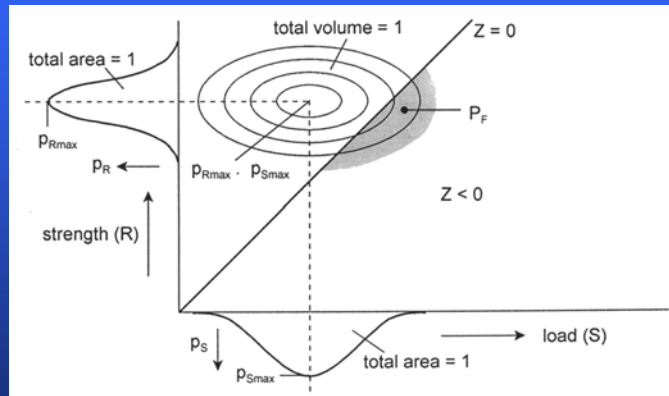
Figure 2.3: Probability Density Function

W

u
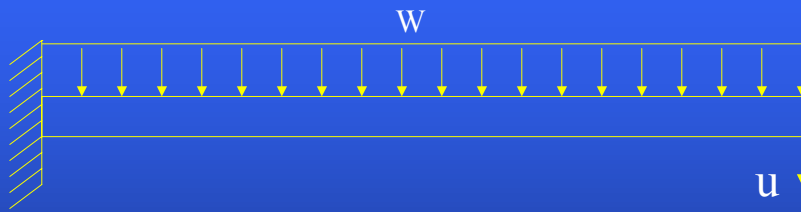
Figure 2.4: Cantilevered Beam

3.   A REVIEW OF PROBABILITY RANDOM FIELDS MODELS FOR SOIL PROPERTIES AND RAINFALL

3.1   Introduction

Slow soil movements, rainfall, soil properties and other geotechnical events exhibit space and time variabilities. These inherent variabilities are continuous and are related from point to point in the space stratum. Thus, the closer the points, the closer the relationships between events at two locations, and vice versa. Analysis of pipeline structural integrity, planning of routes and decisions related to pipeline inspection; repair and maintenance involve the use of characteristic values of the above-mentioned events. Experimental measurements are usually executed at selected discrete locations in the space stratum to obtain characteristics values of the events. The high cost of experimentation and the difficulty with measuring values of an event at all locations requires that the measured values be characterized such that "true" representations of the event at all locations in the continuum can be readily extracted.

Probability techniques, namely, random variable and random field models have been used in the literature to represent events with variabilities. A random variable model of a space dependent event such as slow soil movement assumes that the event has the same statistical values, namely, mean and variance at all locations. The model also assumes that there is no relationship between statistical values of the event at various locations and that the event can be effectively represented by a single mean value and a single mean value and a single variance. Thus, the model does not acknowledge the existence of spatial variability, implying that a spatial event such as slow soil movement can be completely characterized by measurements taken at a single location. The model is, therefore, unrealistic, inaccurate and can be overly conservative (Vanmarcke, 1983).

This has given birth to the use of random fields that realistically account for spatial variability in modeling these events. A random field can be defined as a family of spatially correlated random variables or random processes. Random fields have been used in modeling and analysis of soil of properties and rainfall. Most of the analysis have focused on homogeneous random fields (Vanmarcke, 1977a, 1977b, 1983; Bowles and Ko 1984; Soulie et al, 1990; Kulhuway et al, 1991; Li and Lumb, 1987; Li and Lo, 1993; Gui et al, 2000, Griffits and Fenton, 1993; Asaoko and Grivas, 1982; de Marsily, 1985; Young, 1984; Tang, 1984; Baecher, 1981;

Christakos, 1987; Yang et al, 1996; White, 1993). Soil Properties such as soil strength, pore pressure, hydraulic conductivity, permeability, porosity, and relative density have all been modeled as random fields. Estimation techniques for characteristic parameters of random fields, such as correlation structures have also been developed (DeGroot and Baecher, 1993; Mardia and Marshall, 1984; 1995). A summary of all the pertinent issues discussed in the afore-mentioned random field paper and other papers on the subject is presented in this section.

3.2 General Representation of a Random Field

The general representation of an event that is space dependent as a random field (DeGroot and Baecher, 1993) is

$$\omega(\hat{r}) = \tau(\hat{r}) + f(\hat{r}) \tag{3.1}$$

where

$\omega(\hat{r})$ is the realization or sample of field at $\hat{r}$

$\hat{r} = \left(x(t), y(t), z(t)\right)$ is the spatial location

$\tau(\hat{r})$ is the trend component of field (commonly referred to as mean value) at $\hat{r}$

$f(\hat{r})$ is the zero trend fluctuating component of field at $\hat{r}$

t is time.

Equation (3.1) represents the realization of a random field at any specified location. Random fields have been classified based on the statistical properties of the field or on the dimension of the field (Vanmarcke, 1983).

3.3 Classification Statistical Properties

Statistical properties are representative values of a field based on the ensembles of various realizations. The statistical properties of a random field $\omega(\hat{r})$ that are of primary interest are the trend, the variance and the autocovariance or autocorrelation function. These properties are defined below:

Trend:

The mean or the trend or average value at $\underset{\sim}{r}$ is given by

$$E[\omega(\hat{r})] = E[\tau(\hat{r})] = \mu(\hat{r})$$
(3.2)

Variance:

The variance of the random field at $\hat{r}$ is given by

$$\text{var}(\omega(\hat{r})) = E[\omega(\hat{r}) - \tau(\hat{r})]^2 = E[f(\hat{r})]^2 = \sigma^2(\hat{r})$$
(3.3)

It is a measure of the average deviation from the trend at $\hat{r}$.

Autocovariance Function or Autocorrelation function:

The autocovariance function of a random field at two locations $\hat{r}$ and $\hat{r}^1$ is given by

$$\text{cov}(\omega(\hat{r}))\omega(\hat{r}^1) = E[((\omega(\hat{r}) - \tau(\hat{r}))(\omega(\hat{r}^1) - \tau(\hat{r}^1)))]$$
$$= E[f(\hat{r})f(\hat{r}^1)]$$
(3.4)

A scaled value of the autocovariance function is the autocorrelation function. Specifically, the autocorrelation function of the field at locations $\hat{r}$ and $\hat{r}^1$ is given by

$$\rho(\hat{r}, \hat{r}^1) = \frac{\text{cov}(\omega(\hat{r})\omega(\hat{r}^1))}{\sqrt{\text{var}(\omega(\hat{r}))}\sqrt{\text{var}(\omega(\hat{r}^1))}}$$
(3.5)

The autocovariance and autocorrelation functions describe the average dependents of values of the random fields at two different locations. The symbols E[.], var[.], cov[r] used in the above equations have the following meaning:

E [.] is the expected value;

var [.] is the variance;

cov[.] is the autocovariance function;

ρ(.) is the autocorrelation function.

Equation 3.2 and 3.3 describe statistical properties at a particular point or location in the field. These properties are commonly referred to as point properties. Equations 3.4 and 3.5 present cross moments between two points in the field and are generally called cross point properties. A random field is completely characterized by its point and cross point properties. The point and cross point properties of a field can be used to classify a field as either homogeneous or non-homogeneous.

3.3.1 A Homogeneous Random Field

A random field is said to be homogeneous when the statistical values of the point properties are constant and the statistical value of the cross-point properties depends only on the distance or separation between point. Specifically, the statistical values of a homogeneous field are given by

$$E[\omega(\hat{r})] = E[\tau(\hat{r})] = \mu \tag{3.6}$$

$$\text{var}(\omega(\hat{r})) = E[\omega(\hat{r}) - \tau(\hat{r})]^2 = E[f(\hat{r})]^2 = \sigma^2 \tag{3.7}$$

$$\text{cov}(\omega(\hat{r})\omega(\hat{r}^1)) = E[(\omega(\hat{r}) - \tau(\hat{r}))(\omega(\hat{r}^1) - \tau(\hat{r}^1))] = = E[f(\hat{r})f(\hat{r}^1)] = \sigma^2 \rho(\hat{r} - \hat{r}^1) \tag{3.8}$$

When the cross point properties, namely autocovariance and autocorrelation is a function of absolute distance between the points, the field is said to be isotropic. That is

$$\text{cov}(\omega(\hat{r}))\omega(\hat{r}^1) = \sigma^2 \rho(|\hat{r} - \hat{r}^1|) \tag{3.9}$$

3.3.2 A Non-Homogeneous Random Field

A random field is said to be non-homogeneous when any of the statistical values of the point or cross point properties is dependent on the location. Specifically, the statistical values of point and cross point properties is given by

$$E[\omega(\hat{r})] = E[\tau(\hat{r})] = \mu(\hat{r}) \tag{3.10}$$

$$\text{var}(\omega(\hat{r})) = E[\omega(\hat{r}) - \tau(\hat{r})]^2 = E[f(\hat{r})]^2 = \sigma^2(\hat{r}) \tag{3.11}$$

$$\text{cov}(a(\hat{r}))a(\hat{r}^1)) = E\left[\left((a(\hat{r}) - \tau(\hat{r}))(a(\hat{r}^1) - \tau(\hat{r}^1))\right)\right] = E[f(\hat{r})f(\hat{r}^1)] = \sigma^2 \rho(\hat{r}, \hat{r}^1) \qquad (3.12)$$

It is noted that the only requirement for a field to be non-homogeneous is that either Equations 3.10, 3.11 or 3.12 is dependent on location. A non-homogeneous random field can be decomposed into a series of homogeneous fields. An alternative classification of a random field is based on the dimension of the field. Four possibilities exist, namely, one-dimensional, two-dimensional, three-dimensional and space-time random field.

3.3.3 Auto Correlation Function of a Random Field

The autocorrelation function or the autocovariance or the cross point property is a measure of a field similarity between the values of the field at two locations. It is reflection of the effect of separation distance on values of field at two locations and it simply states that values of a field at two points close to each other are likely to be similar while values for points remote from each other are likely to be independent of each other. The autocorrelation function is a distinguishing feature of a random field and must, therefore, be characterized for the field. Two indices of correlation, namely, scale of fluctuation (Vanmarcke, 1983) and autocorrelation distance (DeGroot and Baecher, 1993) have been used to describe the degree of similarity or correlation. The autocorrelation distance is defined as the distance r_o to which the autocorrelation function $\rho(\hat{r})$ decays to $\dfrac{1}{e}$ while the scale of fluctuation, δ, is defined as

$$\delta = \int_0^\infty \rho(r)dr \qquad (3.13)$$

is a measure of the distance within which the random field shows relatively strong similarity with itself. The values of the field at location lying within a distance ρ of each other are both likely to be above or below the trend. Thus, a small ρ implies rapid fluctuation about the trend and a large reduction in variance. Autocorrelation functions can be 1, 2 or 3 dimensional. Various functions have been used to model autocorrelation and are generally of the exponential form.

3.4 Estimation Technique for Autocorrelation Structure

Various methods for estimating the statistical properties of a random field (DeGroot and Baecher, 1993), namely, trend, variance and correlation function have been reported in the literature. The methods can be classified into three categories namely:

(i) Method of Moments;
(ii) Blue linear Unbiased Estimators;
(iii) Maximum Likelihood Estimators.

These methods have been applied in the literature (DeGroot and Baecher, 1993) to homogeneous random fields. Summary review of the methods is presented in the following sections for the sake of completeness.

3.4.1 Method of Moments

This method employs the moments of the realizations of a random field to estimate its statistical values. It is the most common method for estimating the statistics of a random field. The method is easy to use for homogeneous random fields. The moment estimators of the mean or trend and the variance of a random field $\omega(\hat{r})$ are:

$$\hat{\mu}_r = \frac{1}{n}\sum_{i=1}^{n}\omega(\hat{r}_i)$$

(3.14)

$$\hat{\sigma}^2 = \frac{1}{n-1}\sum_{i=1}^{n}\left(\omega(\hat{r}_i) - \hat{\mu}_r\right)$$

(3.15)

The moment estimator of the autocovariance function of a homogeneous random field measured at uniform intervals along one dimension is:

$$\hat{c}[d] = \frac{1}{N-d}\sum_{i=1}^{N-d}\left(\omega_i(r_i) - \hat{\mu}_r\right)\left(\omega(r_{i+d}) - \hat{\mu}_r\right)$$

(3.16)

where $\hat{\mu}_r$ is given by Equation 3.14 (or by a trend removal from the data), d is the lag distance between pairs of observations and N-d is the number of data pairs separated by d. At lag distance d=0, Equation 2.16 reduces to the variance of the data set. It is a non-parametric technique in that no assumption is made on the form of the autocovariance function.

3.4.2   Best Linear Unbiased Estimators

Best linear unbiased estimators (BLUE) are used to make point estimates of a homogeneous random field using a weighted combination of existing measurements. It is a form of stochastic interpolation. A linear estimator, $\overline{\omega}(\hat{r}_i)$, of the random field $\omega(\hat{r}_i)$ is chosen such that:

$$\overline{\omega}(\hat{r}_i) = \sum_{i=1}^{h} w_i \omega(\hat{r}_i) \qquad (3.17)$$

such that

$$\sum_{i=1}^{h} w_i = 1 \qquad (3.18)$$

where n is the number of observation of the random field property $\omega(\hat{r})$, $\omega(\hat{r}_i)$ is the i-th observation of the random field property at location $\hat{r}_i$ and is the w_i is the weighting factor assigned to the i-th observation. The estimator $\hat{\omega}(\hat{r}_i)$ becomes a BLUE estimator if the weights, w_i, are determined by a three-step procedure (Spikula, 1983):

Step 1: Apply the unbiased condition, thereby restricting the w_i such that:

$$\sum_{i=1}^{h} w_i = 1 \qquad (3.19)$$

Step 2: Determine the estimator variance $\hat{\sigma}_\omega^2(\hat{r})$, for the estimator $\hat{\omega}(\hat{r}_i)$ of the true random field property at location $\hat{r}^*$

$$\hat{\sigma}_\omega^2 = E\left[\left(\omega(\hat{r}) - \omega(\hat{r}^*)\right)^2\right] \qquad (3.20)$$

$$= \sum_{i=1}^{n}\sum_{j=1}^{n} w_i w_j c(\hat{r}_i, \hat{r}_j) - 2\sum_{j=1}^{n} w_i c(\hat{r}_i, \hat{r}^*) + c(\hat{r}^*, \hat{r}^*) \qquad (3.21)$$

where $c(r_i, r_j)$ is the autocovariance of ω between points $\hat{r}_1$ and $\hat{r}_j$

Step 3: Minimize Equation 3.21 over all w_i subject to equation 3.20.. This yield optimal values of w_i and the BLUE estimator

BLUE estimators can be used indirectly to estimate the parameters describing the autocovariance function of a random field. The method is parametric in that the shape of the autocovariance function must be assumed. Usually two parameters are used to define the function, (1) $r_\circ$, the autocovariance distance, and (2) b, the ratio of spatial variability to the variance of the data set. For example, using these two parameters the exponential autocovariance function is written as

$$c[d] = b_\sigma^2 e^{-d/r_\circ}$$

(3.22)

The objective of the method is to select the optimal values of $r_\circ$ and b .

Once the form of the autocovariance function is assumed, each observed value is iteratively removed from the data set and then estimated from the remaining n-1 data points. This is performed for a given combination of $r_\circ$ and b . For each estimate, two statistics are computed:

1. Estimation Error

$$\varepsilon = \hat{\omega}(r_i) - \omega(r_i)$$

(3.23)

2. Error Ratio

$$ER = \frac{\varepsilon}{\sqrt{\hat{\sigma}_\omega^2 + \sigma_n^2}}$$

(3.24)

where σ_n^2 is equal to the noise component of the variance $\left(\hat{\sigma}_\omega^2(1-b)\right)$. For each combination of b and $r_\circ$, n values of ε and ER are computed. Minimizing the variance of ε yields the optimal value of $r_\circ$ while minimizing the variance of EF yields optimal value of b.

3.4.3   Maximum Likelihood Estimators

Maximum likelihood estimators are found by considering the possibility of having observed the data $\underline{x} = \{x_1, x_2, ..., x_n\}$, conditioned on possible values of the parameter(s) θ to be estimated. θ is a vector of the parameters defining the autocovarince function. The method takes as an estimate that value of θ, which provides the greatest probability of having observed $\underline{x}$, as

calculated from the joint probability distribution of the observations.

For example, take the case of a random variable X for which the form of the probability density function $f(x \mid \theta)$ is known. If the parameter θ, which defines the function $f(x \mid \theta)$ is also known, then the joint probability of a random sample $\underline{x} = \{x_1, x_2, ..., x_n\}$ of X is given by:

$$f_{x_1, x_2, ..., x_n}^{(x_1, x_2, ..., x_n \mid \theta)} dx_1 dx_2 ... dx_n$$

$$= fx_1(x_1)dx_1 f_{x_2}(x_2)dx_2 ... f_{x_n}(x_n)dx_n \tag{3.25}$$

$$= \prod_{i=1}^{n} f_x(x_1 \mid \theta)dx \tag{3.26}$$

However, the parameter θ is not known; θ is the parameter we wish to estimate from the observations $\underline{x}$. On the other hand, the outcomes $\underline{x} = \{x_1, x_2, ..., x_n\}$ are known, and thus Equation 3.26 can be considered a function only of θ, and it gives the relative likelihood (i.e., the relative probability of having observed the sample $\underline{x}$. This is the joint likelihood function of the sample and is more commonly written as

$$L(\theta \mid x_1, x_2, ..., x_n) = \prod_{i=1}^{n} f_x(x_i \mid \theta) \tag{3.27}$$

The maximum likelihood estimator $\hat{\theta}$ of θ is found by selecting the value of $\hat{\theta}$ which maximizes the likelihood function (Benjamin and Cornell, 1970).

One common method used to solve for the maximum likelihood estimator is to differentiate the likelihood function and set it equal to zero. Since it is easier to differentiate a sum than a product, one generally prefers to work with the log likelihood function:

$$Ln[L(\theta \mid x_1, x_2, ..., x_n)] = Ln[L(\theta \mid \underline{x})] \tag{3.28}$$

$$= Ln\left[\prod_{i=1}^{n} f_x(x_i \mid \theta)\right] \tag{3.29}$$

$$= \sum_{i=1}^{n} Ln\{f_x(x_i \mid \theta)\} \tag{3.30}$$

The method can also be generalized to estimate a vector of parameters, $\underline{\theta} = \left(\theta_1, \theta_2, ..., \theta_n\right)$, by selecting the vector of estimates $\underline{\hat{\theta}} = \left(\hat{\theta}_1, \hat{\theta}_2, ..., \hat{\theta}_n\right)$ which maximizes the log likelihood function $LL(\underline{\theta} \mid \underline{x})$,

$$Ln\left[L(\underline{\theta} \mid x_1, x_2, ..., x_n)\right] = \sum_{i=1}^{n} Ln\left[f_x\left(x_i \mid \underline{\theta}\right)\right]$$

(3.31)

3.4.4   Limitations of Current Random Field Models

Unfortunately, all of the soil properties/rainfall random field models reviewed for purposes of this project have limitations that make them unsuitable for slow soil movement. These limitations include:

(i)   They only have spatial variability and the effect of time is ignored;

(ii)   The spatial variability is usually assumed to be homogeneous, that is, the mean value of the field is the same at all locations. However, for soil movement, the average values depend on locations; thus, the need for a non-homogeneous random field model; and

(iii) The models do not consider or recognize the existence of variation of field characteristics with changes in seasons.

Decomposing the data into a series of seasonal (or monthly) time series is a relatively easy way to remove the seasonal trends from the original time series. For rainfall and snowfall data this means that the original time series data can be partitioned into twelve monthly random variables, each with its own unique set of statistical properties. Slope movement data can be handled in a similar fashion, although random fields must be used to represent monthly slope movement in order to account for the spatial dependence of slope movement.

Long term trends refer to systematic changes in the mean rainfall/ground movement over a period of time. The general practice when investigating long term trends in seasonal data is to calculate and compare successive yearly averages. It should be noted, however, that what is considered "long term" is relative, and depends on the extent to which data is available. For example, if rainfall data is available for 100 years, it may be possible to observe eleven year

cycles. However, if data is available for only ten of fifteen years, the same eleven-year cycle could only be detected as a long-term trend. In practice, long-term features are usually defined as those that span more than a fifth of the length of the available data. For the present study, since most sites have rainfall records for the past fifty or more years, long-term features are roughly 10 years in length.

In the event that long-term trends can be established in the data, it is recommended that the series be partitioned, or decomposed, into periods corresponding to the length of the trends (in a manner similar to what was done with corrosion depth in PRESAP phase I).

4. A REVIEW OF STOCHASTIC FINITE ELEMENT METHODS

4.1 Introduction

The finite element method (FEM) has been a successful tool in solving engineering problems including soil mechanics problems (Britto and Gun, 1987). However, the deterministic FEM has several limitations especially for soil pipeline problems. For example, soil properties, such as soil strength, pore water pressure and hydraulic conductivity, which exhibit a great deal of spatial variability are usually modeled as deterministic constants without regard to their variance and spatial correlation and this could limit the applicability of the result. In order to overcome the limitations of deterministic finite element methods, stochastic finite element methods (SFEM) that apply probability theory have been developed. A review and summary of the various stochastic finite element formulations is the focus of this chapter .

Stochastic finite element methods can be broadly classified into four groups:

(i)   Perturbation based SFEM approach;

(ii)   Reliability based SFEM approach;

(iii)   Response Surface Methods;

(iv)   Monte Carlo Simulation Methods; and

4.2 Perturbation-Based SFEM Approach

The perturbation approach to probabilistic structural analysis was introduced about two decades ago. Initial applications were directed at the study of the eigenvalue problem related to the free vibration of structures with stochastic mass and stiffness matrices and the solutions of linear static problems involving loading and system stochasticity. The work of Hisada and Nakagiri (1985) represents one of the modern applications of this approach to structural safety and reliability analysis. In that work, SFEM was applied for the evaluation of the reliability index and design point within the framework of the Advanced First-Order Second Moment (AFOSM) method.

Consider the linear finite element equation

$$KU = F \tag{4.1}$$

where K is the global stiffness matrix, U is the vector of nodal displacement and F is the global nodal

load vector. These stochastic quantities can be expressed as

$$K = K_0 + \Delta K$$
$$U = U_0 + \Delta U \qquad (4.2)$$
$$F = F_0 + \Delta F$$

where K_0, U_0 and F_0 are considered to be deterministic parts and the increments ΔK, ΔU and ΔF are considered to be the stochastic parts of K, U, and F, respectively. Substituting Equations (4.2) into (4.1) gives

$$[K_0 + \Delta K][U_0 + \Delta U] = [F_0 + \Delta F]. \qquad (4.3)$$

on neglecting the product ($\Delta K \Delta U$) and separating the deterministic and stochastic parts of Equation (4.3) gives:

$$K_0 U_0 = F_0 \qquad (4.4)$$

and

$$K_0 \Delta U = \Delta F - \Delta K U_0 \qquad (4.5)$$

Equation (4.4) gives the finite element solution at the deterministic expansion point. From the solution of Equation (4.5), the second-order variation of the response may be computed.

A more rigorous and general formulation of the perturbation approach can be constructed using Taylor series expansion. This also paves the way for higher-order approximations. The stiffness matrix in Equation (4.1) may be expanded about a deterministic stake as:

$$K = K_0 + \sum_{i=1}^{n} K_i'(x - x_i) + \frac{1}{2} \sum_{i=1}^{n} \sum_{j=1]}^{n} K_{ij}'(x - x_i)(x - x_j), \qquad (4.6)$$

where K_i' and K_{ij}' are the first-order and second-order partial derivatives of the stiffness matrix with respect to the basic variables X. The displacement and load vectors in Equation (4.1) may be expanded in a similar fashion and the response computed as previously described.

When the mean state is chosen as the expansion point the approach is referred to as the

mean-centred perturbation approach. Using mean-centred perturbation results in the computation of reliability indices according to the First-Order Second Moment (FOSM) approach of structural reliability analysis. In the AFOSM, however, the performance function is expanded not about the mean values of the basic variables, but about the most probable failure point. Hisada and Nakagiri (1985) utilized this approach and also presented a second-order perturbation formulation. A notable feature of the formulations is that the stiffness matrix is inverted only once in contrast to simulation or response surface methods in which many inversions of the stiffness matrix are required. The key to successful solution using the perturbation approach is the ability to compute and assemble partial derivative matrices for stiffness, displacements, and loads. Second-order approximations are obviously more accurate than the first-order approximations; however, these involve the computation and assembly of second-order partial derivative matrices.

Numerous applications of the perturbation approach have been reported in the open literature. Prominent in this connection are the works of Liu et al. (1986,1988), in which applications were investigated for linear and nonlinear structural dynamics and a variational formulation of probabilistic finite elements established.

Although the formulation of the perturbation approach is mathematically elegant, its application to reliability analysis has several disadvantages. The mean-centred perturbation method suffers from invariance problem associated with FOSM. Furthermore, the perturbation methods do not use the distribution information about the basic random variables, even if it is available. This is a serious limitation, unless for the exceptional cases in which all the variables are normally distributed. The method is also not capable of producing accurate results when there are large variations in the random variables defining a problem.

4.3   The Reliability-Based SFEM Approach

Current methods for reliability analysis compute the reliability index β by solving the limit state equation g(X)=0 explicitly. However, search algorithms that do not rely on an explicit solution of the limit state equation are available. These algorithms only need the value and the gradient of the performance function at each iteration point.

The reliability based SFEM approach has been formulated and applied for several structural problems by Der Kiureghian and his co-workers. Der Kiureghian and Ke (1988, 1985) used the first-order reliability method for static analysis of linear structures with random properties and in Igusa and Der Kiureghian (1988) applied the method to dynamic analysis. In a more recent work Liu and Der Kiureghian (1991), a general framework for reliability based SFEM analysis based on FORM and SORM was presented. New expressions for the required gradients of the response of geometrically nonlinear structures were derived and implemented. This work represents the first application of the finite element reliability method (FERM) in conjunction with SORM with non-Gaussian random fields, and with system reliability analysis. Arnbjerg-Nielsen and Bjerager (1988) and Mahadevan (1988) has also developed and implemented a reliability-based SFEM approach and applied it to the modelling of frame structures.

The reliability approach has a significant advantage over the perturbation approach in that information about the distribution of the random variable is used. Furthermore, in the reliability approach, the probability density function of the response variable (not just second moment statistics) can be obtained. Since the computation of response gradients is a key operation in the implementation of this procedure, the use of the adjoint method has been recommended for this operation (Liu and Der Kuireghian, 1991 and Reh at al, 1991). This technique is estimated to be capable of reducing computation times by a factor equal to the number of random variables. The reliability-based approach to SFEM structural reliability analysis is especially compatible with the algorithmic structure of existing FEA codes.

4.4   Response Surface Methods

The response surface method is a classical statistical technique in which a complex (computer) model is approximated by a simple functional relationship between the output quantities and the input (basic) variables. The approximation is usually based on polynomial functions and, often, linear or quadratic response functions are applied. Adopting the simpler response functions allows an efficient repeated computation, for example, as may be needed in simulations or parameter studies in structural reliability analysis. This is because the approximation to the response surface rather than the original limit state function is used in the calculation of failure probabilities.

The concept of response surface methods has been used when approximating costly to compute and/or non-differentiable limit state functions. Within the framework of the stochastic finite element method, the steps required for the implementation of the response surface technique were described by Favavelli (1989). This involves the application of regression analysis to obtain the polynomial coefficients involved in the representation of the limit state function using the results of several numerical experiments.

The explicit representation of the limit state function g(x), for the quadratic approximation for example, takes the form:

$$\bar{g}(x) = a + \sum_{i=1}^{n} b_i \, x_i + \sum_{i=1}^{n} \sum_{j=1}^{n} c_{ij} \, x_i \, x_j \qquad (4.7)$$

where n is the number of basic random variables (x_i) and the coefficients a, b, and c are to be determined from numerical experiments.

The works of Schuëller et al. (1991), and Bucher and Bourgund (1990) are among recent efforts at promoting the application of response surface methods. The work of Böhm and Brückner-Foit (1990), in particular, introduced a special lack of fit measure and formulated criteria for accepting response surface models in structural reliability analysis. Ghanem and Spanos (1990) proposed a Galerkin-based response surface approach in which the surface is approximated by its projection onto a complete set of polynomials that are orthogonal to the Gaussian measure. These polynomials are known as polynomial chaos functions and are believed to be capable of yielding accurate approximations of the response surface.

So far, no general scheme has been developed to efficiently establish linear and quadratic response surfaces for reliability computations. Further research is needed to establish general, efficient, and robust response surface methods for reliability analysis. Nevertheless, this methodology appears to be a promising tool for large scale structures.

4.5   Monte Carlo Simulation Methods

The direct Monte Carlo simulation method was used in many early works in stochastic finite element analysis. In this simple method, deterministic analysis is carried out for a series of parameters generated in accordance with their probability distribution. The desired statistics of the response quantities, such as the mean, variance, and exceedance probabilities, are then evaluated based on the generated sample sets/space. Applications of this procedure can be found in Vanmarcke et al. (1986) and Takada (1991).

The Monte Carlo simulation method has the advantage that it is adaptable to all types of problems and the results can be obtained to desired accuracy. However, for practical problems with many random variables or small failure probabilities this procedure is usually too expensive, since a large number of solutions are needed to obtain reliable results. Shinozuka and his co-workers (1988) have introduced the Neumann (Monte Carlo simulation) expansion technique. Computation time for this technique is reduced significantly since only the mean stiffness matrix needs to be decomposed with this formulation. Other schemes have also been proposed to improve the efficiency of the simulation method. However, for pipeline soil interaction, this procedure is not recommended.

5. **REVIEW OF RANDOM FIELD MODELING APPLICATIONS IN GROUND MOVEMENT STUDIES**

5.1 **Introduction**

The great majority of published reports related to random field modeling of ground movement have focused on the spatial and temporal variation of earthquake ground motions (see Fenton and Vanmarcke, 1991, Harichandran and Vanmarcke, 1986). During the course of this review, only a few studies were found which had any direct relevance to the current study (i.e. slow slope movement or creep). Of particular note are a series of papers/reports published by Grivas et. al. (1995, 1996, and 1998), who used a probabilistic methodology to analyze landslides and their effects on the safety of buried pipelines. While this work did not use a random field modeling approach, it is still relevant because, in addition to the use of probabilistic methods, Grivas developed a phenomenological model linking slope creep movement to environmental factors such as precipitation.

In addition to Grivas' work, Evgin (1997) reviewed the current state-of-the-art and identified research needs that would improve the methods of analysis used in the current design practice of assessing the integrity of pipelines in creeping slopes. Although the Evgin report is not strictly focused on the use of random field modeling for slow slope movement, the background information it contains and the accompanying recommendations it makes are quite relevant to the present study.

In the sections which follow, brief reviews of both Evgin's findings and Grivas' work will be presented.

5.2 **Slow Slope Movement**

As Evgin describes, slow slope movement of natural slopes is a well-known, complex, and time dependent phenomenon. The main purpose of Evgin's work was to identify the research needs for cost-effective design of pipelines buried in creeping slopes. As part of this work a comprehensive list of factors causing slope movements were identified and summarized below:

1. Creep

2. Change in pore pressure due to intense rainfall or rapid snowmelt

3. Erosion or excavation at the toe of the slope

4. Freeze-thaw cycles

5. Weathering

6. Change in groundwater level

7. Tectonic uplift and glacial rebound

8. Temperature variations

Of these factors, Evgin focused most of his literature review work on creep effects and the changes that take place in pore water pressure due to rainfall.

As mentioned above, the objective of Evgin's work was to identify the research needs that would improve analysis methods used in assessing the structural integrity of pipelines in creeping slopes. Based on his review Evgin made the following suggestions:

1. Develop a 3-D finite element program capable of simulating the slope movements and predicting pipeline strains. Use environmental loads such as rainfall and temperature changes as direct input into the calculations.

2. Develop and validate constitutive relations for cyclic creep in soils and soil-structure interfaces for natural soils under both saturated and unsaturated states. Use wetting and drying cycles for the unsaturated state. For the saturated condition, alternate the pore water pressure between two values to simulate the groundwater fluctuations in slopes.

3. Develop a stochastic finite element modelling capability.

5.3   Phenomenological Based Modeling

In a series of studies, Grivas et. al. (1995, 1996, and 1998) developed probabilistic models to analyze landslides and their effects on the safety of buried pipelines. In one particular study involving the case of the Simonette River crossing (Grivas (1995)), ground movements were divided into two groups: (1) instantaneous movements, (2) gradual movements. The instantaneous movement represented the failure case. The factor of safely for the stability of the slow moving slopes, the annual rate of movement, M, was expressed as a function of the annual precipitation, R as:

$$M = 0.089R + 0.48$$

where the units for both M and R were mm/year. It was assumed that the accumulated ground movements would be hazardous to the pipeline if the reached a given threshold level. The probability of the ground movements exceeding a specified value was determined.

Grivas (1997), through his association with Arista International, also participated in a research and development project sponsored by both NOVA Gas Transmission Ltd. (now TransCanada Pipelines) and the National Energy Board of Canada. The process used in that study diverged from traditional landslide analysis procedures in three important aspects, namely:

1. It focused on gradual ground movement
2. It was concerned with the analysis of numerous sites distributed over large geographical areas where only limited data was available
3. It used phenomenological modeling, rather than mechanistic or kinematic approaches, to predict ground movement.

According to the authors of the Arista report, traditional techniques for predicting ground movement are based on standard slope stability analysis methodologies and/or extrapolation of monitored slope performance data.   When the goal is to analyze numerous sites located across large areas, the traditional approach becomes infeasible. The authors go on to suggest that phenomenological models offer an alternative approach. Using this technique, a perceived

cause (rainfall) is mathematically related to an effect (ground movement), without attempting to model the mechanics of the relationship. This approach allows for the prediction of movement based solely on rainfall.

In order to develop the relationship between slope movement and rainfall, the Arista researchers used the relatively extensive historical movement and rainfall measurements and other data available for the few instrumented (slope indicators) sites to develop rainfall-movement prediction models that can be generalized at new (unmonitored) sites where very little geotechnical information is known,

The approach adopted by Arista was comprised on three key components:

1. Rainfall data analysis.
2. Movement data analysis.
3. Site-specific rainfall-movement modeling.

The objective of the rainfall analysis process was to generate a composite rainfall record for a specific site. Essentially this involved computing a weighted average of rainfall amounts recorded at weather stations neighboring the specific site of interest. Once this composite rainfall time series record was generated, the Arista software (SLIDER) then perform a series of statistical checks (i.e.: elimination of redundant weather stations) and analyses (i.e.: temporal analysis of the composite rainfall record).

In the Arista movement analysis phase, movement data from various inclinometers available at the site of interest is used to generate a composite movement record. Additional processing is also performed in order to estimate a series of other slope parameters, including the associated slip surface, the rate and magnitude of movement, and the direction of movement.

In rainfall-movement modeling phase culminates in the development of models which can be used to predict ground movement based on rainfall values. The first step in this stage of the analysis is establishing whether the movement and rainfall data sets are amenable for modeling. The second step involves what the authors call "quantification of the similarities between rainfall and ground movement data sets. This essentially involves computing

correlation and cross-correlation coefficients for the rainfall and ground movement data. In the third step, empirical and time-series models are fitted to the data. In the fourth and final step of the analysis, cross-validation techniques are used to assess the accuracy of the predicted slope movement and estimate uncertainties in the modeling.

5.3.1   Limitations of Arista Model

Overall, the rainfall/slope movement modelling technique developed by Arista appears to be an excellent tool for predicting rainfall induced soil movement. Unfortunately, there appears to be some limitations inherent in the way "composite" time series records are created. By performing a simple weighted average, it is not clear how non-homogeneity in the data is accounted for in the Arista model. In the PRESAP code, for example, a technique known as MCM (Multi-Component Mapping technique) has been adopted in order to systematically account for non-homogeneity when generating composite data samples (generating sample data at locations where data was not previously available). Without a similar approach, the methodology used in Arista's SLIDER code may be limited to slopes having homogeneous rainfall and slope movement data.

6. **PRESAP PRECIPITATION – SOIL MOVEMENT MODELLING REQUIREMENTS**

This chapter provides a description of the software requirements to be addressed in order to provide a precipitation/ground movement random field modelling capability within the PRESAP system. In general, the requirements for this new PRESAP modelling capability are essentially the same as the original (i.e.: database management, data characterization, system definition, and reliability assessment – see Figure 6.1), however some new requirements have been added in order to address the limitations associated with the other techniques proposed in the literature (i.e.: spatial non-homogeneity and seasonal dependence).

6.1 **Database Management**

The main tasks to be performed by the PRESAP database manager will include the following:

1. Extraction of monthly precipitation and soil movement time series data from formatted ASCII files;

2. Interaction with the other components of the PRESAP system (i.e.: retrieving/storing precipitation and ground movement data);

3. Decomposition of the time series data into 12 monthly random variables/fields (i.e.: rainfall data for a particular site must be decomposed into random variables representing rainfall for January, February, March, etc.);

It is anticipated that the decomposition of the time series data will lead to statistically stationary monthly random processes (i.e.: a time series having statistical properties, such as mean, variance, and autocorrelation, that are not a function of time). A conversion to stationary processes means, in effect, that seasonal trends in the original data have been removed.

At the suggestion of the Scientific Authority, a web site maintained by the Climate Monitoring and Data Interpretation Division of the Climate Research Branch of the Meteorological Service of Canada (http://www.cccma.bc.ec.gc.ca/hccd/) will be used as the source for precipitation data. An example of the format of this data is provided in Figure 6.2. Data representing ground movements recorded at individual inclinometers will also be expected to follow this general format.

6.2 Data Characterization

In order to satisfy the data characterization requirements of the precipitation/ground movement analysis tool, a number of statistical analyses must be performed on the data, including:

1. Calculation of statistical properties (mean and variance);
2. Distribution fitting (i.e.: what form of distribution best fits the data – normal, lognormal, Rayleigh, etc.);
3. Organization of ground movement data into random variables;
4. Computation of correlation coefficients between individual random variables;
5. Computation of the correlation structure for non-homogeneous random fields using the MCM technique;
6. Computation of cross correlation between different variables (i.e. rainfall and ground movement);
7. Generating samples of random variables (or fields) at locations where data had not been collected;

Subroutines originally developed for use in Martec's probabilistic software tools COMPASS (LIU (1999)) and PRADAC (LIU (1997)) will be used extensively in order to satisfy the numerical modelling requirements listed above.

6.2.1 MCM Technique

Due to the fact that the MCM method was designed to compute the statistical properties

(including the correlation structure) of non-homogeneous random fields, it will address the one of the most serious limitations inherent in other soil modelling algorithms.

In order to gain an appreciation for the versatility of the MCM technique, consider Boissieres' (1992) case study involving a non-homogeneous field. The field under consideration is a square domain consisting of two rectangular regions (each having a unique set of statistical properties): a lower region (R1) corresponding to the area below the line $y \leq 3.5$ and an upper region (R2) corresponding the area above the line $y > 3.5$. The correlation structure used in this example is provided below in Equation 6.1.

$$\rho(P_1(x_1,y_1),P_2(x_2,y_2)) = \begin{cases} e^{-\sqrt{a(x_1-x_2)^2+b_1(y_1-y_2)^2}}, & y_1 \leq 3.5, y_2 \leq 3.5 \\ e^{-\sqrt{a(x_1-x_2)^2+b_2(y_2-y_1)^2}}, & y_1 > 3.5, y_2 > 3.5 \\ e^{-\sqrt{a(x_1-x_2)^2+b_1(3.5-y_1)^2+b_2(y_2-3.5)^2}}, & y_1 \leq 3.5, y_2 > 3.5 \\ e^{-\sqrt{a(x_1-x_2)^2+b_2(3.5-y_1)^2+b_1(y_2-3.5)^2}}, & y_1 > 3.5, y_2 \leq 3.5 \end{cases} \qquad (6.1)$$

where $a = 0.15, b_1 = 0.3$ and $b_2 = 0.2$

Comparisons of the correlation results are provided below in Figures 6.5 and 6.6, and appear to show excellent agreement between with Boissieres' published results.

It is also important to note that the MCM method can be used to estimate the mean and variance at locations in the field where data has not been pre-defined. For example, consider a one dimensional random field defined by 10 random variables positioned along the x-axis starting at location x = 0 and terminating at location x = 9 (see Figure 6.7). The mean value of the field is defined using the following expression:

$$Mean = \frac{x}{4}, \qquad\qquad \text{for } 0.0 \leq x \leq 5.0$$

$$Mean = 1 + \frac{(x-5)}{4}, \qquad\qquad \text{for } 5.0 < x \leq 9.0$$

The MCM predictions for the mean value along the x-axis are provided below in Figure 6.8, and show excellent agreement with the prescribed values.

6.3   Model/System Definition

Users' of the PRESAP precipitation/ground-movement code must be able to perform two basic types of analyses:

1. Computation of the probability of event occurrence (i.e.: the probability that November rainfall will exceed 100 mm and slope movement at location x-y-z is less than 5 cm);

2. Computation of the conditional probability of occurrence (i.e.: what is the most likely value for ground movement in June if rainfall in May is less than 10 mm).

6.4   Reliability Assessment

In the reliability assessment phase of the analysis, Monte Carlo simulation will be used to compute both the probability of event occurrence and the conditional probability of occurrence. As discussed in section 2.2 of this report, Monte Carlo simulation is an indirect way of integrating the joint probability density functions and solving for the probability of failure for the system.

6.4.1   Computing the Probability of Occurrence

For cases involving the computation of the probability of occurrence, the algorithms developed for PRESAP must be able to compute the probability of failure for parallel systems. An example of such a system is provided below in Figure 6.9. For this type of analysis, the individual limit state functions are relatively simple to define: the first limit state function defines failure as June rainfall amounts exceeding 5 mm, while the second limit state function defines failure as September ground movement for site location $P(x, y, z)$ failing below 3 cm.

The combination of these two limit state functions amounts to computing the probability that September ground movement at location $P(x, y, z)$ will exceed 3 cm when rainfall amounts for June are less than 5 mm.

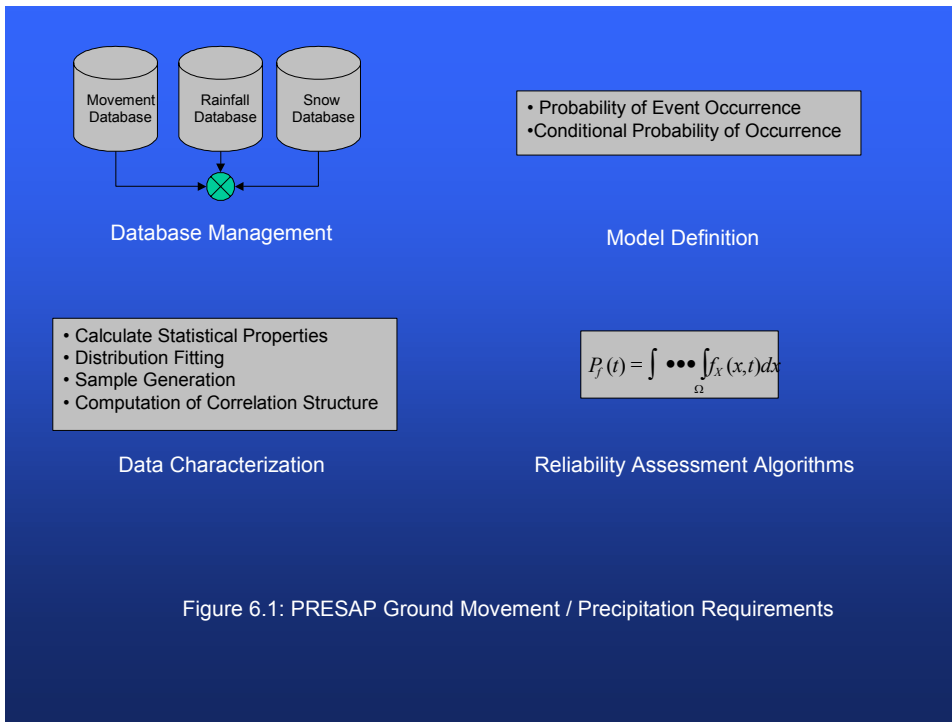### 6.4.2   Computing the Conditional Probability of Occurrence

By way of extension, the techniques used above to estimate the probability of occurrence can also be used to compute the conditional probability of occurrence of a random variable. As an example consider the steps involved in attempting to calculate the most likely value for ground movement during the month of May at a particular site $P(x, y, z)$, given rainfall amounts at the same for the month of March and April which are less 5 mm. First, a large number of samples (N) must be generated for all three variables used to define the system. The computation of these samples requires that distributions for each random variable must be available, and that the correlation between each variable must also be established. Once the samples have been generated, they are filtered according to the whether they satisfy the limit state functions used to define the system. Next, the samples satisfying the conditions defined in the system limit state function are then sorted according to the ground movement value. Once the samples are sorted a conditional probability density function can be established.

6.4.3   Sample Generation

It is clear from the computational requirements listed above that the ability to generate realizations of correlated random variables (either as individual random variables representing different quantities or as collections of random variables representing a single random field) is a key element in the computational process. In order to provide this capability within PRESAP, a covariance matrix decomposition procedure has been proposed. The basic steps involved in this process include:

1. Generation of the covariance matrix R_{XX}, where R_{ij} represents the correlation between random variable i and random variable j;

2. Transformation of the covariance matrix R into standard normal space ($\overline{R}$) using the Natif method;

3. Computation of the eigenvector matrix H and diagonal eigenvalue matrix S of $\overline{R}$.

4. Transformation the random variables (X) into standard normal form (U);

5. Using a random number generator, compute the realizations of the independent standard normal form of the random variables;

6. Application of the linear transformation equation $X = \mu_x + \sigma_x HSU$ in order to obtain realizations of the correlated random variables X (where μ_x represents the mean vector of X and σ_x represents the variance matrix of X);

7. Using the inverse transformation technique, convert the samples generated in step 6 into the original distribution used to represent the random variables.

Figure 6.1: PRESAP Ground Movement / Precipitation Requirements

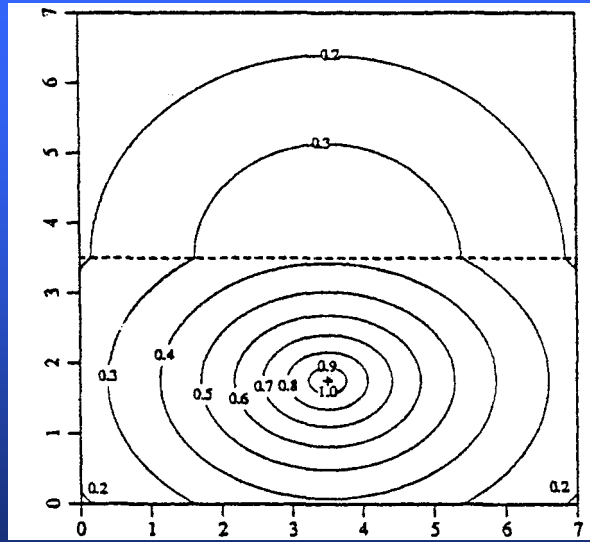Figure 6.2: Sample of Rainfall Data From Web Site

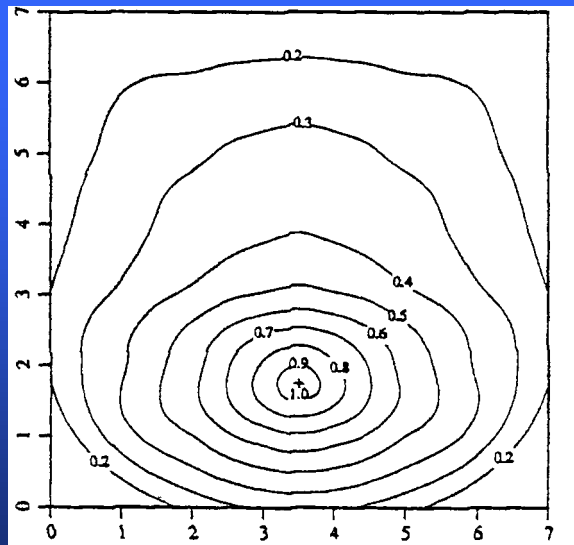Figure 6.3: Non-homogeneous Random Field (Reproduced from Boissieres)

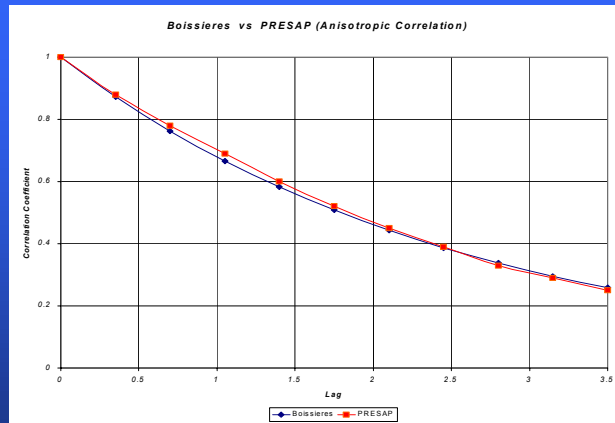Figure 6.4: Contour Plot of Correlation Structure Computed by Boissieres for Location (3.5,1.75)

Figure 6.5: Comparison Between Correlation Structure Computed by *PRESAP*

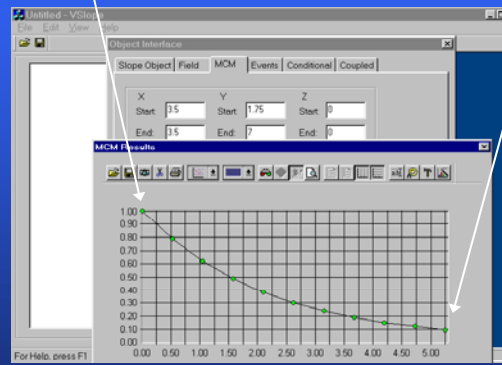and Boissieres - Between Locations (x=3.5,y=1.75) and (x=3.5, y=5.25)

Figure 6.6: Correlation Structure Computed by *PRESAP*

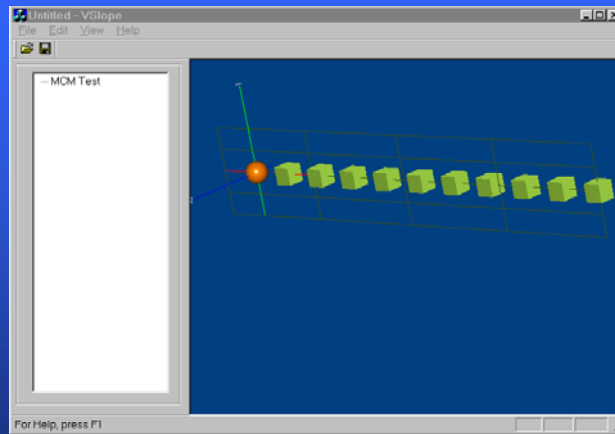Between Locations (3.5,1.75) and (3.5, 6.75)

Figure 6.7: One Dimensional MCM Test Case Modeled Using *PRESAP* (Screen Capture of Actual Code)
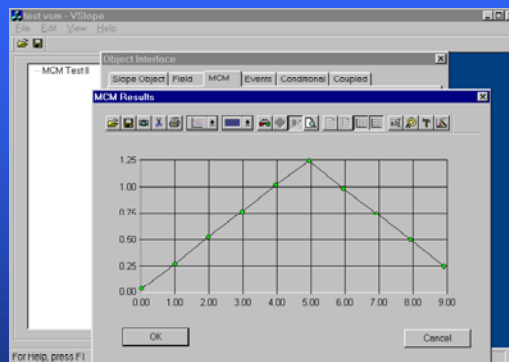

Figure 6.8: Mean Value Distribution Predicted by *PRESAP* (Screen Capture of Actual Code)
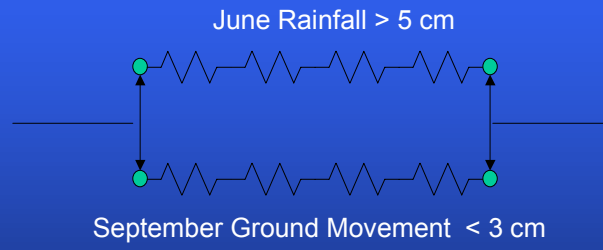
Figure 6.9: Probability of Occurrence Limit State Functions

7.   SOFTWARE DESIGN

This chapter provides a description of the software designed to address the precipitation/ground movement functional requirements listed in the previous chapter.

7.1   Software Development Tools/Environment

Due to the experience of the project team, the Microsoft developers' studio (http://msdn.microsoft.com/) was used as the software development platform for this study. In general, all new code was written in C++, and compiled using Microsoft's Visual C++ compiler. In order to avoid any language incompatibility problems with the legacy FORTRAN codes, all subroutines and functions extracted from Martec's COMPASS and PRADAC programs were assembled into a series of dynamic link libraries (DLL's).

In order to provide user's with a convenient means for manipulating the slope movement and precipitation data, a windows-based graphical user interface for the prototype code has been developed. In order to take full advantage of the tools supplied with the Visual C++ compiler, all new classes were derived from one of two base classes: CObject or CObArray. CObject is the principal base class for the Microsoft Foundation Class Library and provides a number of basic services, including:

1. Serialization (I/O) support;
2. Run-time class information;
3. Object diagnostic output;
4. Compatibility with collection classes.

The CObArray class supports the management of CObject pointers. These object arrays are similar to C language arrays, but have additional functionality which allow them to dynamically shrink and grow.

7.2   Class Hierarchy

Figure 7.1 provides a class hierarchy chart for the new slope stability classes. Near the top of the chart is the CSlopeObject class. For the purposes of this application, CSlopeObject acts as a base class, providing all classes derived from it with all the basic functionality of CObject plus additional graphics capabilities (i.e.: drawing and picking).

Also near the top of the hierarchy chart is the SceneGraph class, which is derived from CObArray. The main responsibility of the SceneGraph class is to provide database management support. All precipitation and ground movement data required for a slope analysis can be accessed via the SceneGraph. User's can gain direct access to the objects stored in the SceneGraph via the SceneGraph interface. This interface (a dockable tool bar) is located on the left-hand side of the PRESAP window frame (see Figure 7.2).

Next on the hierarchy chart are a series of classes derived from CSlopeObject and used to represent random variables and random fields. The *CRanVariable* class has been designed to act as a generic random variable object capable of representing either rainfall, snowfall, or ground movement. Some of the principle attributes of this class are: an array of "raw" data variates, a reference to a COMPASS distribution object (COMPASS supports up to seventeen different distribution types), plus a number of statistical properties (i.e.: mean, variance, etc.).

The most important methods developed for the *CRanVariable* class are related to the computation of the random variable statistics (mean and standard deviation) and correlation with other random variables. In addition to these, random variables developed for use in *PRESAP* also have the ability to generate a series of realizations. These realizations are based on the fitted distribution type (i.e.: normal or lognormal). The code responsible for generating these samples was modified from routines originally developed for use in Martec's *COMPASS* software. It was anticipated that the ability to generate samples of random variables (either in groups or individually) would be an effective means for computing conditional probabilities for cases involving multiple random variables contained within random fields.

In addition to the features listed above, the *CRanVariable* class can be assigned global x-y-z coordinates. As a result, the instances of this class can be graphically displayed (see Figure 7.2).

The *CRanField* class has been designed to act as a generic random field / random process object. Both rainfall and snowfall can be represented as individual random processes, each consisting of twelve random variables (a single random variable corresponding to each month of the year). Essentially, random field objects will be instantiated as collections of random variables. Most of the functionality built into this class is focused on managing the child random variable objects, i.e.:

1. adding new random variables to the field;
2. deleting random variables from the field;
3. providing users with access to the attributes of individual random variables;
4. generating samples/realizations of the random variables;
5. initializing the statistical properties of the population of random variables;
6. modifying/prescribing the correlation structure;
7. creating a grid-work of new random variables;
8. graphically displaying the random variables contained in the field;
9. Computing the joint probability of a set of random variables;
10. Computing the conditional probability of a particular random variable.

7.2.1 *CSlopeField* Class

Like precipitation data, slope movement data may be represented by a series of monthly slope movement objects. However, because of the spatial dependence of slope movement data, a collection of 12 random fields should be used to manage the slope movement data The *CSlopeField* class has been developed to manage all slope movement data used in the slope stability analysis. The individual random fields, representing slope movement for each of the twelve months, can be accessed through the property pages of the interface property sheet developed for the *CSlopeField* class (see Figure 7.3).

7.2.2 *CCoupledField* Class

In order to manage all precipitation and slope movement data, a *CCoupledField* class has been implemented into the *PRESAP* code. The *CCoupledField* class has three principal attributes:
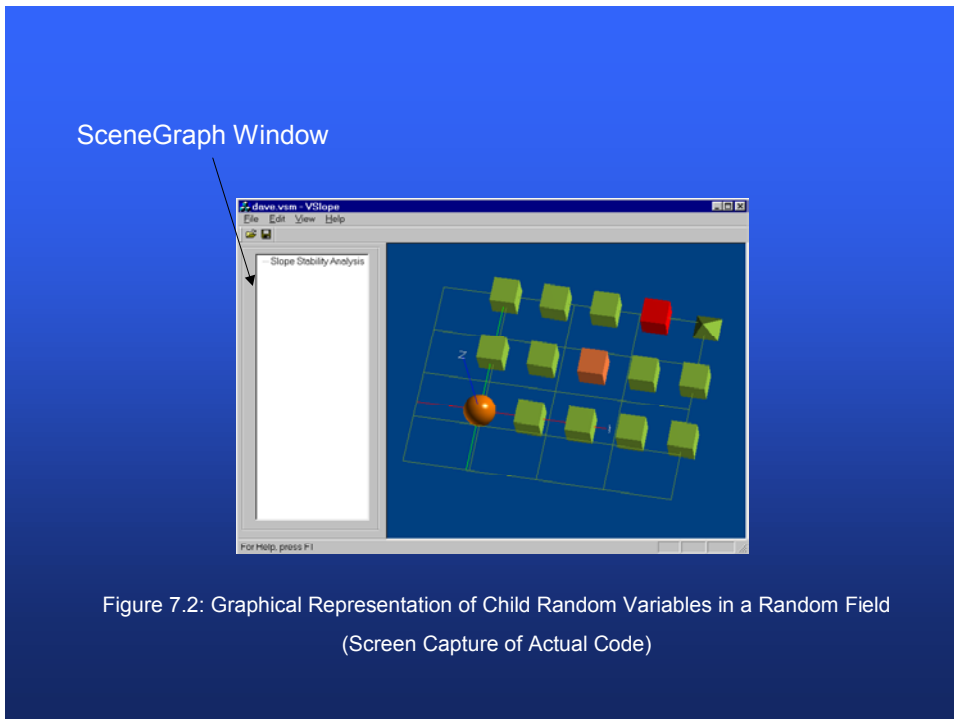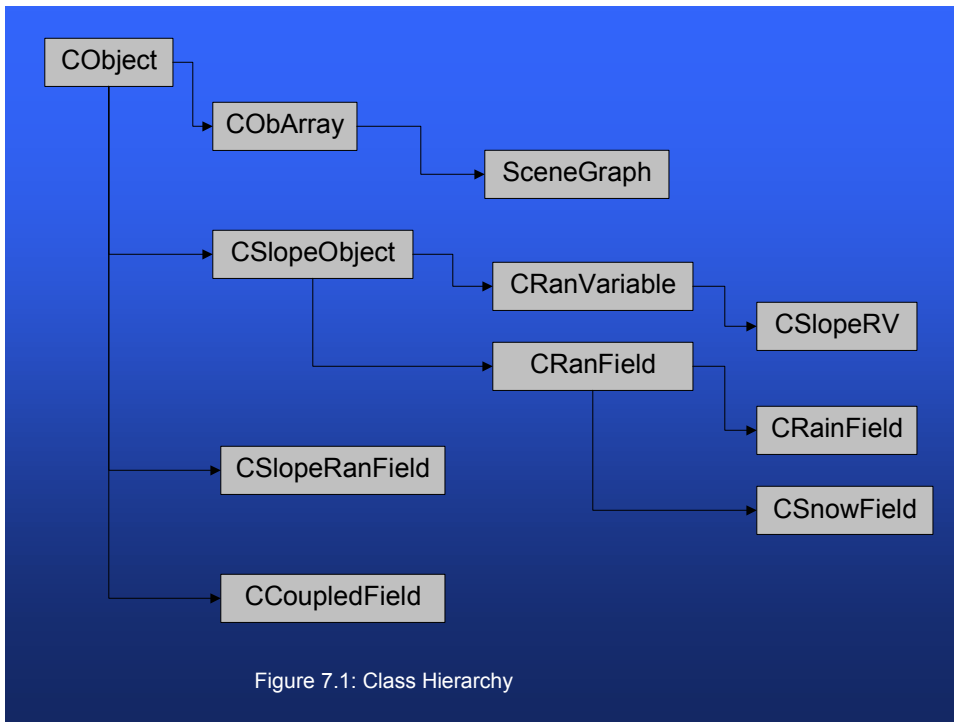
1. A *CSlopeField* object responsible for managing the slope movement data.
2. A *CRainField* object responsible for managing the rainfall data.
3. A *CSnowField* object responsible for managing snowfall data.

The interface property sheet designed for the *CCoupledField* class provides quick access to the data stored in each of the three attributes described above (see Figures 7.4 and 7.5).

7.2.2.1 *CCoupledField* Class Functionality

In its present state, the functionality of the *CCoupledField* class is limited to one key method: computing the conditional probability of slope movement given input related to either rainfall, snowfall, or both. In order to accomplish this task, the *VSlope* code allows the user to select the months of rainfall and snowfall (see Figure 7.6) to include in the conditional slope movement probability calculations (the default is for the user to include all months of rainfall and snowfall). Following this selection, the user can then define the month and location at which the conditional slope movement estimate is to be computed (see Figure 7.7).

During the implementation of the *CCoupledField* class difficulties arose when attempting to compute correlation between different random fields (i.e.: slope movement and rainfall data). It is important to note, however, that computing correlation between random fields is only a problem at locations where "raw data" is not available. However, when attempting to compute correlation at locations where raw data is not available, the method developed for use in this project modelled correlation between precipitation and slope movement, as a function of position. For example, if we are interested in establishing the correlation coefficient between the September rainfall random variable and the November slope movement at a location x-y-z, we could estimate this correlation coefficient as a weighted average of the correlation at neighboring locations (see Figure 7.8). Note that the correlation at these neighboring locations can be calculated because raw data is available at these sites. The calculation of this weighted average can be performed using tools already developed for the project, namely the MCM method

Figure 7.1: Class Hierarchy

SceneGraph Window

Figure 7.2: Graphical Representation of Child Random Variables in a Random Field
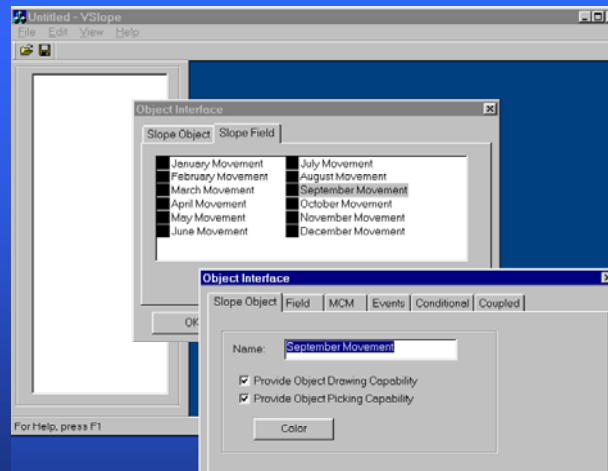
(Screen Capture of Actual Code)

Figure 7.3: Interface Property Sheet Representing the *CSlopeField* Class (Screen Capture of Actual Code)
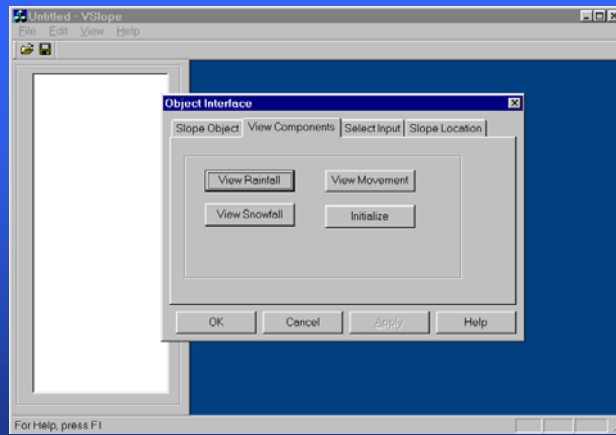

Figure 7.4: Interface Property Sheet Developed for the *CCoupledField* Class (Screen Capture of Actual Code)
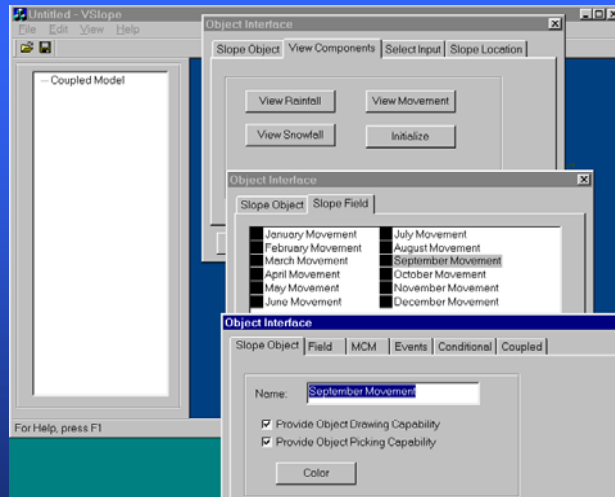
Figure 7.5: Accessing Slope Movement Random Field Data (Screen Capture of Actual Code)
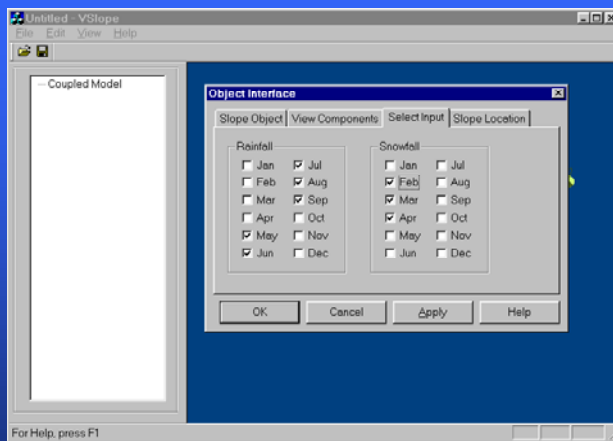
Figure 7.6: Selecting the Precipitation Data to be Used in the Conditional Probability Calculations

Figure 7.7: Defining the Particular Slope Location to be Considered in the Conditional Probability Analysis

Figure 7.8: Computing Precipitation Correlation Coefficients at Locations Where Raw Data is not Available

$$\rho_X = f(\rho_1, \rho_2, \rho_3, \rho_4, \rho_5, \rho_6)$$

Figure 7.8: Computing Precipitation Correlation Coefficients at Locations Where Raw Data is not Available

8. ILLUSTRATIVE EXAMPLES

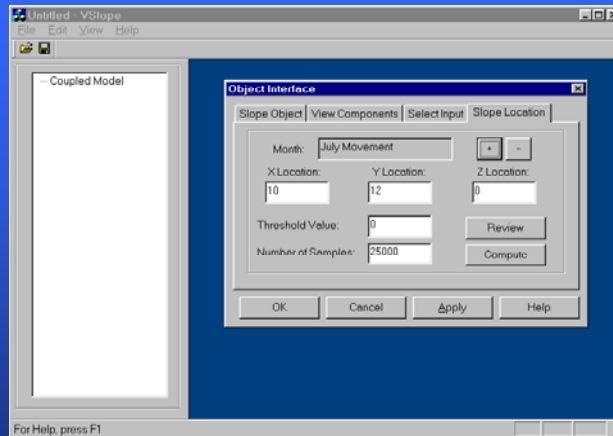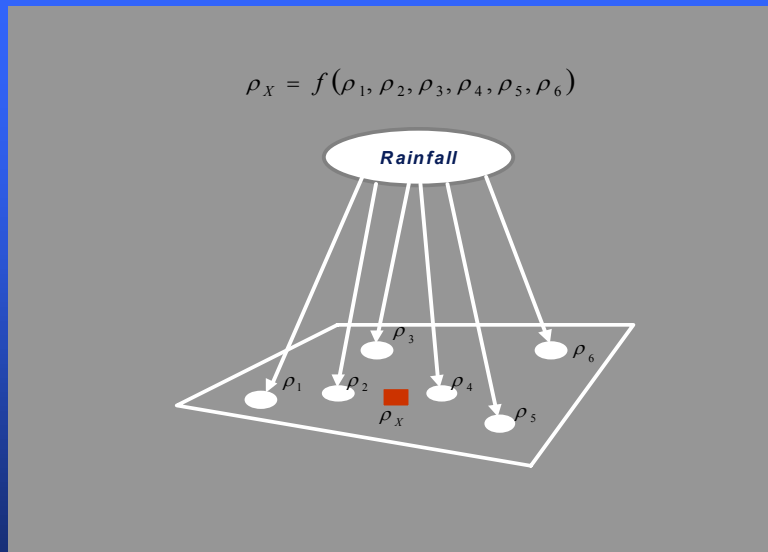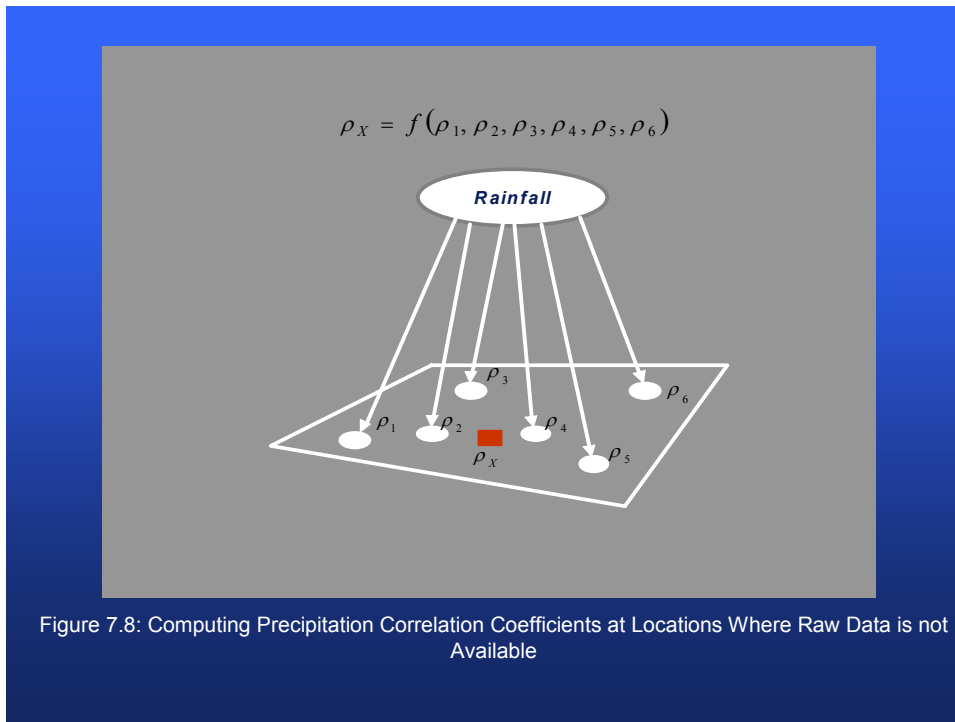In order to demonstrate how the new ground movement analysis code can be used in practice, consider the slope represented in Figure 8.1. The overall length and height of the slope is 100 m and 10 m respectively. Slope indicator positions are hi-lighted by green dots.

For the purposes of this example, we wish to establish how the expected ground movements for the month of June vary with changes in April rainfall amounts. Table 8.1 provides a list of the simulated statistical properties for each of the 11 slope indicators plus the rainfall (April rainfall amounts were assumed to be constant over the area of interest). All variables are assumed to behave as lognormally distributed random variables

Table 8.1: Statistical Properties of Slope Model Random Variables

Variable	Mean (cm)	Standard Deviation	Correlation with Rain
Slope Indicator 1	5.42	0.542	0.33
Slope Indicator 2	4.78	0.478	0.36
Slope Indicator 3	7.02	0.702	0.4
Slope Indicator 4	8.50	0.850	0.45
Slope Indicator 5	9.40	0.940	0.5
Slope Indicator 6	12.86	1.286	0.55
Slope Indicator 7	11.82	1.182	0.60
Slope Indicator 8	13.76	1.376	0.67
Slope Indicator 9	14.58	1.458	0.74
Slope Indicator 10	16.84	1.684	0.81
Slope Indicator 11	19.19	1.919	0.9
April Rainfall	10.00	1.000	1.0

For the purposes of this demonstration, slope movement estimates where modelled using two different rainfall scenarios: April rainfall less than or equal to 8 cm and April rainfall less than or equal to 12 cm. Figure 8.2 provides the numerical estimates for the most likely slope

movements generated by PRESAP for both cases. As expected, the PRESAP phenomenological model of the rainfall and ground movement predicts an increase in expected ground movement with increasing levels of rainfall. Ninety-five percent confidence levels for both cases are provided in Figures 8.3 and 8.4 respectively.
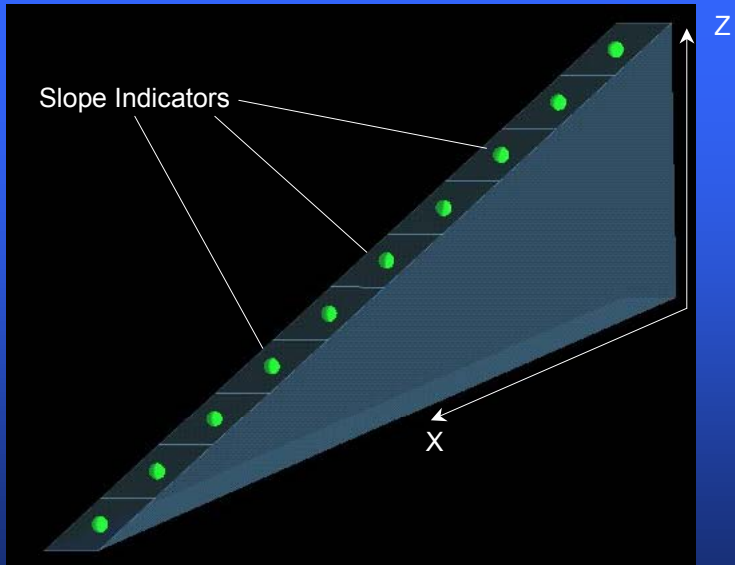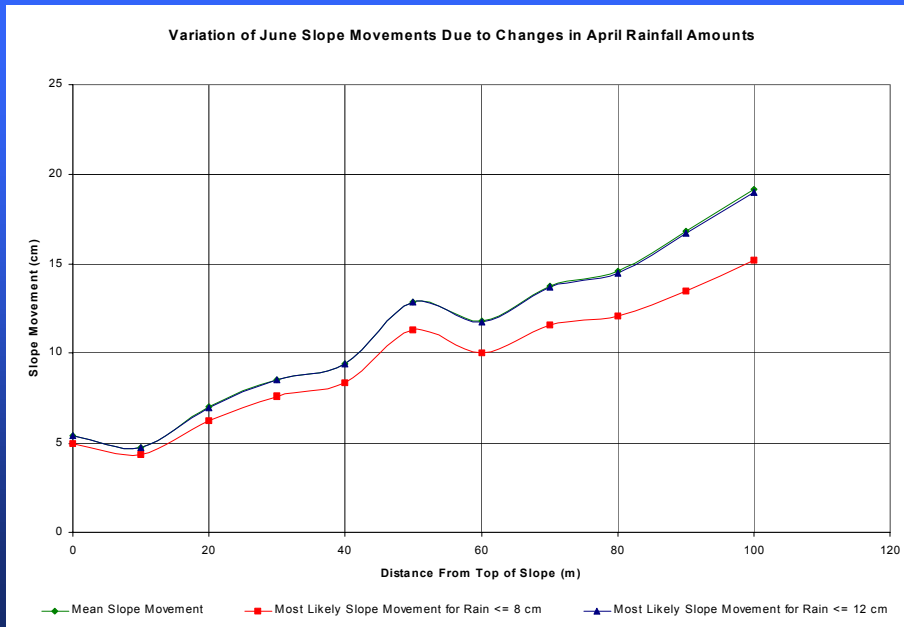
Figure 8.1: Simulated Slope Geometry

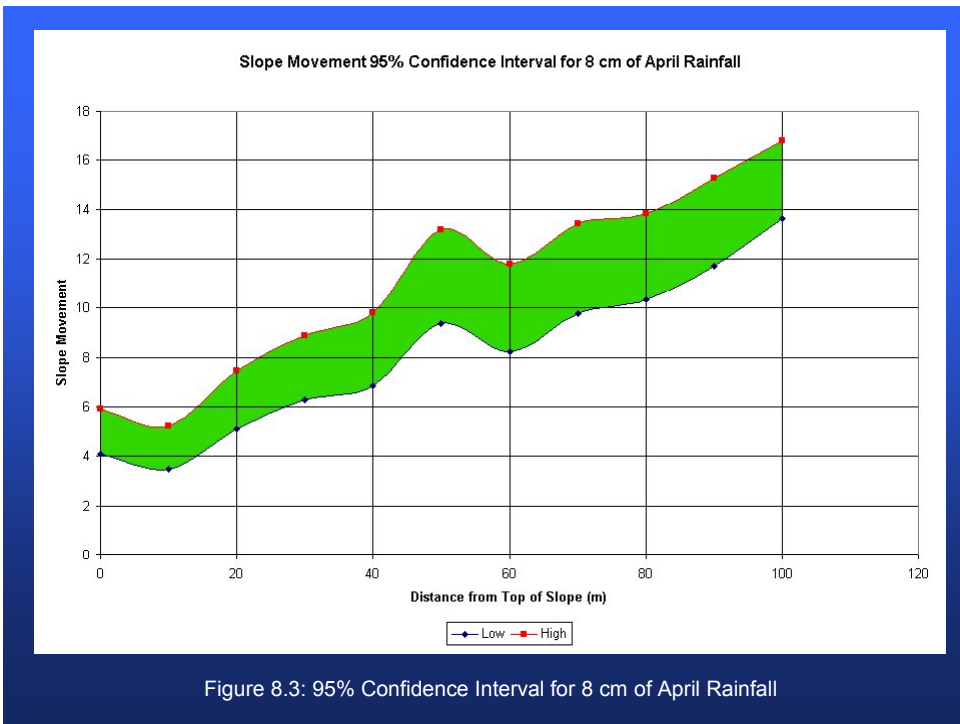Figure 8.2: Variation in Slope Movement Due to Changes in Rainfall

Figure 8.3: 95% Confidence Interval for 8 cm of April Rainfall
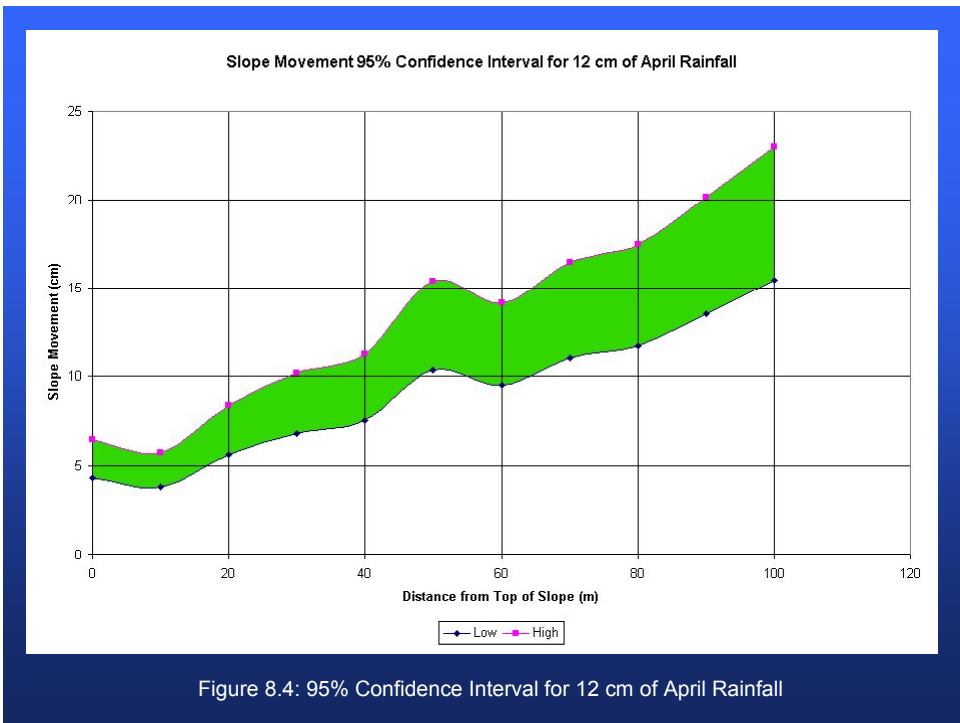
Figure 8.4: 95% Confidence Interval for 12 cm of April Rainfall

9.   RECOMMENDATIONS AND CONCLUSIONS

During the course of this present work the probabilistic modelling software tool PRESAP has been upgraded in order to provide random field modelling of precipitation induced slow slope movement. It is anticipated that this new modelling capability will provide the pipeline industry and government regulators with a software tool capable of (1) modelling the relationship between precipitation and slope movement for particular pipeline routes and (2) predicting the likelihood of exceeding thresholds for slope movement for various levels/intensity of precipitation.

Continued development of the PRESAP program is of importance in order to provide and maintain a state-of-the-art computational tool in the field of probabilistic random field modelling of pipeline hazards. Some considerations for the next phase of development are listed below.

1. Application to seabed mobility;
2. Application to ice scour;
3. Modelling of permafrost;
4. Incorporation of stochastic finite element methods;
5. compare slope movement estimates generated by PRESAP with data collected by the pipeline industry.

10.   REFERENCES

1.   E. VANMARCKE, Random Fields: Analysis and Synthesis, The MIT Press, Cambridge, Massachusetts (1983).

2.   E. VANMARCKE, Probability Modeling of Soil Profiles, ASCE Journal of Geotechnical Engineering, vol 103(11), pp. 1227-1246 (1977a).

3.   E. VANMARCKE, Reliability of Earth Slopes, ASCE Journal of Geotechnical Engineering, vol 103(11), pp. 1247-1265 (1977b).

4.   K. S LI and P. LUMB, Probabilistic Design of Slopes, Canadian Geotechnique, vol 24. pp. 520-535 (1987).

5.   J. YANG, R. ZHANG and M. B. ALLEN, Some Stochastic Analysis of Adsorbing Solute Transport in Two-Dimensional Unsaturated Soil, Water Resource Research, val 329, pp. 2747-2756 (1996).

6.   M. SOULIE, P. MONTES and V. SILVESTRI, Modelling Spatial Variability of Soil Properties, Canadian Geotechnical Journal, vol 27, pp. 617-630.

7.   D. J. DeGroot and G, B, Baecher, Estimating Autocovariance of In-situ Soil Properties, ASCE Journal of Geotechnical Engineering, vol 119(1), pp. 147-166 (1991).

8.   G. A. FENTON and D. V. GRIFFITHS, Statistic of Free Flow through Stochastic Dams, ASCE Journal of Geotechnical Engineering, vol 121(6), pp. 427-436 (1996).

9.   D. V. GRIFFITHS and G. A. FENTON, Seepage beneath Water Retaining Structure Founded on Spatially random Soil, Geeotechnique, vol 43(4), pp. 577-587 (1993).

10.   S. GUI, R. ZHANG, J. TURNER and X. XUE Probabilistic Slope Stability with Stochastic Soil Hydraulic Conductivity, ASCE Journal of Geotechnical Engineering, vol 126(1), pp. 1-9 (2000).

11.   D. BOWLES, H. Y KO (eds). "Probabilistic Characterization of Soil: Bridge Between Theory and Practice, Proceeding of Symposium Sponsored by ASCE geotechnical Division (1984)

12.   W. WHITE, Soil Variability: Characterisation and Modelling, Proceeding probabilistic Methods in Geotechnical Engineering,, Rotterdam, 1993, pp 111-120.

13.   K. S. LI and S.-C. LO eds. Probabilistic Methods in Geotechnical Engineering, Rotterdam, 1993.

14.   A. ASAOKA and D. A. GRIVAS, Spatial Variability of the Undrained Strength of Clay, ASCE Journal of Geotechnical Engineering, vol 108(5), pp. 743-756 (1982).

15. G. de MARSILY, Spatial Variability of Properties in Porous Media: A Stochastic Approach, Advances in Transport Phenomena in Porous Medis, Boston, pp 719-769, 1985.

16. R. N. YOUNG, Probabilistic Nature of Soil Properties, Probabilistic Characterization of Soil: Bridge Between Theory and Practice, Proceeding of Symposium Sponsored by ASCE geotechnical Division pp 19-55, (1984)

17. W. H. TANG, Principles of Probabilistic Characterization of Soil Properties, Probabilistic Characterization of Soil: Bridge Between Theory and Practice, Proceeding of Symposium Sponsored by ASCE geotechnical Division pp 74-89, (1984).

18. G. B. BAECHER, Optimal Estimators for Soil Properties, ASCE Journal of Geotechnical Engineering, No 107, (1981).

19. G. CHRISTAKOS, A Stochastic Approach in Modeling and Estimating Geotechnical Data, International Journal Numerical and Analytical and Method in Geomechanics, vol. 11, pp. 77-102, 1987.

20. E. VANMARCKE, Random Fields: Analysis and Synthesis, The MIT Press, Cambridge, Massachusetts (1983).

21. E.H. VANMARCKE and M. GRIGORIU, "Stochastic Finite Element Analysis of Simple Beams," ASCE, Journal of Engineering Mechanics, Vol. 109, No. 5, pp. 1203-1214, (1983).

22. A. DER KIUREGHIAN and J.B. KE, "The Stochastic Finite Element Method in Structural Reliability," Probabilistic Engineering Mechanics, Vol. 3, No. 2, pp. 83-91 (1988).

23. P.L. LIU and A. DER KIUREGHIAN, "Finite-Element Reliability of Geometrically Nonlinear Uncertain Structures," ASCE, Journal of Engineering mechanics, Vol. 117, No. 8, pp. 1806-1825 (1991).

24. T. HISADA and S. NAKAGIRI, "Role of the Stochastic Finite Element Method in Structural Safety and Reliability", in: Proceedings of the 4th International Conference on Structural Safety and Reliability (ICOSSAR '85), Kobe, Japan, I. Konishi, A.H.-S. Ang, and M. Shinozuka, Eds., pp. I-385 - I-394 (1985).

25. W.K. LIU, T. BELYTSCHKO, and A. MANI, "Random Field Elements," International Journal for Numerical Methods in Engineering, Vol. 23, pp. 1831-1845 (1986).

26. M. LAWRENCE, "Basis Random Variables in Finite Element Analysis," International Journal for Numerical Methods in Engineering, Vol. 24, pp. 1849-1863 (1987).

27. P.D. SPANOS and R. GHANEM, "Stochastic Finite Element Expansion for Random Media," ASCE, Journal of Engineering Mechanics, Vol. 115, No. 5, pp. 1035-1053 (1988).

28.   R. GHANEM and P.D. SPANOS, <u>Stochastic Finite Elements: A Spectral Approach</u>, Springer Verlag, New York, (1991).

29.   G. DEODATIS, "Weighted Integral Method I: Stochastic Stiffness Matrix," ASCE, Journal of Engineering Mechanics, Vol. 117, No. 8, pp. 1851-1864 (1991).

30.   G. DEODATIS and M. SHINOZUKA, "Weighted Integral Method. II: Response Variability and Reliability," ASCE, Journal of Engineering Mechanics, Vol. 117, No. 8, pp. 1865-1877 (1991).

31.   W.K. LIU, T. BELYTSCHKO, and A. MANI, "Probabilistic Finite Element Methods for Nonlinear Structural Dynamics," Computer Methods in Applied Mechanics and Engineering, Vol. 56, No. 1, pp. 61-81 (1986).

32.   W.K. LIU, G.H. BESTERFIELD, and T. BELYTSCHKO, "Variational Approach to Probabilistic Finite Elements," ASCE, Journal of Engineering Mechanics, Vol. 114, No. 12, pp. 2115-2133 (1988).

33.   A. DER KIUREGHIAN and B.-J KE, "Finite-Element Based Reliability Analysis of Frame Structures," Proceedings of the 4th International Conference on Structural Safety and Reliability (ICOSSAR '85), Kobe, Japan, I. Konishi, A.H.-S. Ang, and M. Shinozuka, Eds., pp. I395-I404 (1985).

34.   T. IGUSA and A. DER KIUREGHIAN, "Response of Uncertain Systems to Stochastic Excitation," ASCE, Journal of Engineering Mechanics, Vol. 114, No. 5, pp. 812-832 (1988).

35.   T, ARNBJERG-NIELSEN and P. BJERAGER, "Finite Element Reliability method with Improved Efficiency by Sensitivity Analysis," In Computational Probabilistic Mechanics, W.K. Liu et al., Eds., Proc. Journ. ASME/SES Applied Mechanics and Engineering Science Conference, Berkeley, California, ASME, New York, NY, pp. 15-26 (1988).

36.   S. MAHADEVAN, "Stochastic Finite Element-Based Structural Reliability Analysis and Optimization," PhD Thesis, Georgia Institute of Technology, Atlanta, Georgia, USA, July (1988).

37.   S. REH, F. BÖHM, and A. BRÜCKNER-FOIT and H. RIESCH-OPPERMANN, "First Order Reliability Analysis Using Stochastic Finite Element Methods," Proceedings of the First International Conference on Computational Stochastic Mechanics, Corfu, Greece, P.D. Spanos and C.A. Brebbia, Eds., pp. 385-394, Computational Mechanics Publications, Southampton, U.K. (1991).

38.   L. FARAVELLI, "A Response Surface Method for Reliability Analysis," ASCE, Journal of Engineering Mechanics, Vol. 115, No. 12, pp. 2763-2781, (1989).

39.   G.I. SCHUËLLER, C.G. BUCHER, and H.J. PRADLWARTER, "On Procedures to Calculate the Reliability of Structural Systems Under Stochastic Loading," in: Computational Stochastic Mechanics, Proceedings of the First International Conference,

P.D. Spanos and C.A. Brebbia, Eds., Computational Mechanics Publications and Elsevier Science Publishers, pp. 59-69 (1991).

40.   C.G. BUCHER and V. BOURGUND, "A Fast and Efficient Response Surface Approach for Structural Reliability Problems," Structural Safety, Vol. 7, pp. 57-66 (1990).

41.   R. GHANEM and P.D. SPANOS, "Galerkian-Based Response Surface Approach for Reliability Analysis," Proceedings of the 5th International Conference on Structural Safety and Reliability (ICOSSAR '89), ASCE, pp. 1081-1088 (1990).

42.   E.H. VANMARCKE, M. SCHINOZUKA, S. NAKAGIRI, G.I. SCHUËLLER, and M. GRIGORIU, "Random Fields and Stochastic Finite Elements," Structural Safety, Vol. 3, pp. 143-166 (1986).

43.   T. TAKADA, "Galerkin Method to Analyze Systems with Stochastic Flexural Rigidity," in: Computational Stochastic Mechanics, Proceedings of the First International Conference, Computational Mechanics Publications and Elsevier Science Publishers, pp. 511-522 (1991).

44.   M. SHINOZUKA and F. YAMAZAKI, "Stochastic Finite Element Analysis: An Introduction," in: Stochastic Structural Dynamics, Progress in Theory and Applications, S.T. Ariaratnam, G.I. Schuëller, and I. Elishakoff, Eds., Chapter 14, Elsevier Applied Science, New York (1988).

45.   G. DEODATIS, W. WALL, and M. SAHINOZUKA, "Analysis of Two-Dimensional Stochastic Systems by the Weighted Integral Method," in: Computational Stochastic mechanics, Proceedings of the First International Conference, Computational Mechanics Publications and Elsevier Science Publishers, pp. 395-406 (1991).

46.   G.S. GOPALAKRISHNA and E. DONALDSON, "Practical Reliability Analysis Using a General Purpose Finite Element Program," Finite Elements in Analysis and Design, Vol. 10, pp. 75-87 (1991).

47.   ORISAMOLU, I.R. (1997), "Probabilistic Residual Strength Assessment of Damaged Pipelines (PRESAP)", Martec Technical Report 97-805-02.

48.   ORISAMOLU, I. R., LUI, Q., and CHERNUKA, M. W. (1995), " Probabilistic Residual Strength Assessment of Corroded Pipelines", Proceedings of the Fifth International Offshore and Polar Engineering Conference, The Hague, The Netherlands, Vol. IV, pp. 221-228, ISOPE, Golden, Colorado, USA.

49.   ORISAMOLU, I. R., BRENNAN, D. P., and AKPAN, U. O. (1999), "Probabilistic Residual Strength Assessment of Damaged Pipelines, Martec Technical Report TR-98-07, submitted to Geological Survey of Canada and Nova Gas

50.   KONUK, I. (1998), Personal communication.

51.   McCARTHY, , D. F. (1998), Essentials of Soil Mechanics and Foundations, Prentice Hall, New Jersey.

52.   VANMARCKE, E. H. (1980), "Probabilistic Stability Analysis of Earth Slopes", Engineering Geology, Vol. 16, pp. 29-50.

53.   GRIVAS, D.A., SCHULTZ, B.C., McGUFFY, V.C, O'NEIL, G., AND RIZKALLA, M. (1995), "Landslide Hazard Analysis for Pipelines: The Case of the Simonette River Crossing". Proc. Of the 14th Int. Conference on Offshore Mechanics and Arctic Engineering, Vol. 5, Pipeline Technology, pp. 79-86.

54.   GRIVAS, D.A., SCHULTZ, B.C.,, O'NEIL, and SIMMONDS, G.R. (1996), "Phenomenological Models to Predict Rainfall Induced Ground Movements". Proc. Of the 15th Int. Conference on Offshore Mechanics and Arctic Engineering, Vol. 5, Pipeline Technology, pp. 355-362.

55.   GRIVAS, D.A., SCHULTZ, B.C., O'NEIL (1998), "Phenomenological Models to Predict Rainfall Induced Ground Movements". Proc. Of the 17th Int. Conference on Offshore Mechanics and Arctic Engineering, Vol. 5, Pipeline Technology.

56.   EVGIN, E (1997),"Research Needs for Cost-Effective Design of Pipelines Buried in Creeping Slopes".

57.   ARISTA INTERNATION (1997), "Landslide Hazard Analysis for Pipelines".

58.   FENTON, G.A. and VANMARCKE, E.H. (1991), "Conditioned Simulation of Local Fields of Earthquake Ground Motion." Structural Safety, Special Issue on Spatial Variation of Earthquake Ground Motion.

59.   HARICHANDRAN, R.S. and VANMARCKE E.H. (1986), "Stochastic Variation of Earthquake Ground Motion in Space and Time". Journal of Engineering Mechanics, Vol. 112, No. 2, February 1986.

60.   BOISSIERES, H.P. (1992), "Estimation of the Correlation Structure of Random Fields", Department of Civil Engineering and Operations Research, Princeton University, Princeton NJ.

61.   McBEAN, G. and EVERALL, M.D. (1998), "Business Plan: Science, Impacts and Adaptation", Environment Canada

62.   MEKIS, E and HOGG, W (1999), "Rehabilitation and Analysis of Canadian Daily Precipitation Time Series", Atmosphere-Ocean, Vol. 37, No. 1, http://ccrp.tor.ec.gc.ca/HCCD2/

63.   LIU, Q, ORISAMOLU, I.R., CHERNUKA, M.W. and LUO, X., "COMPASS User's Manual: Version 1.4." Martec Limited, June 1999

64.   LIU, Q., LEVY, R.B. and MA, K.T., "PRADAC: A Probabilistic Aircraft Data Characterization System", Martec Technical Report TR-97-21, 1997

65.   F. H. KULHUWY, M. J. S. ROTH and M. D. GRIGORIU, Some Statistical Evaluation

of Geotechnical Properties, Proceeding 6th ICASP CERRA, Mexico,. pp. 705-712 (1991).

APPENDIX A1: Computing the Likelihood of Event Occurrence

An essential element of the slope stability analysis is the ability to estimate the probability of occurrence for a prescribed event (i.e.: the probability that November rainfall will exceed 100 mm and slope movement at location x-y-z for December will exceed 5 cm). For example, suppose a random field is populated by two random variables: X and Y. If the distributions for both variables are known, and the correlation between the two is also known, it is then possible (in theory) to establish their joint probability density function. Once this is established, the joint probability density function can be used to calculate the probability that, for example, X lies between the threshold values A and B, and Y lies between the threshold values C and D. For the special case where both X and Y have standard normal distributions, this probability calculation can be performed by solving the following integral equation:

$$F(X,Y) = \frac{1}{2\pi\sqrt{1-\rho^2}} \int\limits_{X=A}^{X=B} \int\limits_{Y=C}^{Y=D} \left(\frac{u^2 - 2\rho uv + v^2}{2(1-\rho^2)} \right) du\,dv$$

Algorithms designed for solving the above integral are available as part of the IMSL numerical toolkit (1990). Unfortunately, a more general algorithm, capable of handling an arbitrary number of input random variables, having distributions other than standard normal, has not been identified. Fortunately, the solution of the joint probability can also be estimated through the use of simulation. The steps involved are actually quite simple. First, a sufficiently large number of realizations representing samples of all the random variables must be generated (say 50,000 samples of each random variable). Following this, each realization is compared to the threshold conditions which define the event (i.e: x > 1.0 and Y < -1.0). Once the evaluation of all samples is complete, the probability of the event occurring can then be calculated by simply dividing the number of realizations satisfying the threshold condition by the total number of samples generated.

Estimating Joint Probabilities Via Simulation

Using the sample generation capability recently developed for *PRESAP*, the joint probability of two random variables was estimated and compared to results computed using the IMSL routines. The case considered involves two normally distributed random variables (X and Y),

both having means of 0.0 and standard deviations equal to 1.0. For the purposes of this example we defined the correlation between the two variables to be 0.9, the lower threshold for X was −10.0, the upper threshold for X was set as 0.0, the lower threshold for Y was set as −10.0, and the upper threshold for Y was set as 1.0. A comparison of the IMSL results and the *PRESAP* results, which show excellent agreement, are provided below in Table A.1. Figure A.1 provides an example of the output provided by *VSlope*.

Table A.1: Comparison between IMSL and *PRESAP* Probability Estimates

Method	Probability
IMSL	0.4993
PRESAP/VSlope: 2000 Samples	0.4990
PRESAP/VSlope: 5000 Samples	0.4996
PRESAP/VSlope: 10000 Samples	0.4984

Extending the estimation of joint probabilities to more than two random variables is relatively straightforward using *PRESAP's* simulation algorithm. For example, consider the procedure required to estimate the joint probability related to the event that rainfall for Halifax in the months of July and August does not exceed 200 mm. This can easily be handle in *VSlope* by setting the upper threshold values for both July and August to 200 (see Figure A.2 for the results).

APPENDIX A2: Computing Conditional Probability Density Functions

By way of extension, we can use the simulation techniques described above to estimate the conditional (or marginal) probability of one random variable given prescribed values for other random variables. For example, consider once again our random field populated with the standard normal variables X and Y. For the purposes of this example, assume that the correlation between the two is 0.7. Given this data we could ask the question, "What is the most likely value of Y if X is less than or equal to 0.0?" One way of answering this question is to estimate what is called the conditional probability density function of Y, or more precisely, the conditional probability density function of Y given X <= 0.0.

As is implied by its name, the conditional probability density function of a random variable is, by definition, a distinctly new probability density function, having its own statistical properties (i.e.: mean and standard deviation). In the example posed above, the mean value of this new (or conditional) probability density function is equal to –0.56. This value was computed using routines supplied from the IMSL library of routines. As a result, the answer to the question,"What is the most likely value of Y given X is less than or equal to 0.0?" can be interpreted as the mean value of the conditional probability density function (in this case – 0.56). In fact, we could also provide additional information, such as confidence bounds and a standard deviation along with the estimate for the mean value because the result (the conditional probability density function) is in the form of a distribution.

Estimating Conditional Probabilities Via Simulation

Just as the joint probabilities can be estimated by simulation, the conditional probability distribution functions can also be computed using simulation. For the case of conditional probability estimates, samples are again generated for all random variables in the population under consideration (for example a single slope movement random variable and 12 rainfall random variables – one for each month of rainfall). It is important to note that in order for the samples to be generated properly, the correlation coefficients between all the random variables must be specified.

Once all the samples have been generated (say 10,000 in total), and thresholds (or conditions) have specified for each of the conditional random variables (in this case the rainfall random variables), each of the 10,000 realizations must be evaluated to see if the conditions for rainfall amounts have been satisfied. In this case there may only be a small fraction of the 10,000 realizations that pass the conditional tests, say 850. Once these 850 realizations have been identified, the slope movement values associated with these realizations can then be used to define the conditional probability density function.

The simulation technique described in the previous paragraph has been implemented into the *PRESAP* code and validated with a number of examples. Once such example involved the two random variable case described above. As was stated, the theoretical value computed for this

example had a mean of –0.56 (no standard deviation was reported). The results computed by *PRESAP* are provided below in Figures A.3 and A.4. The mean estimated by *PRESAP* was –0.55, very close to the exact.

As a second example, consider the case where the conditional probability of slope movement for a particular field location is desired for the month of September. The random variable representing this slope movement has a mean value of 10 cm and a standard deviation of 1 cm (fictional data). Using the rainfall data for Halifax, *VSlope* was used to compute the conditional slope movement probability given that rainfall for the month of July was twice the "normal" amount. Estimates for the conditional slope movement probability, computed by *VSlope*, are provided below in Figure A.5.
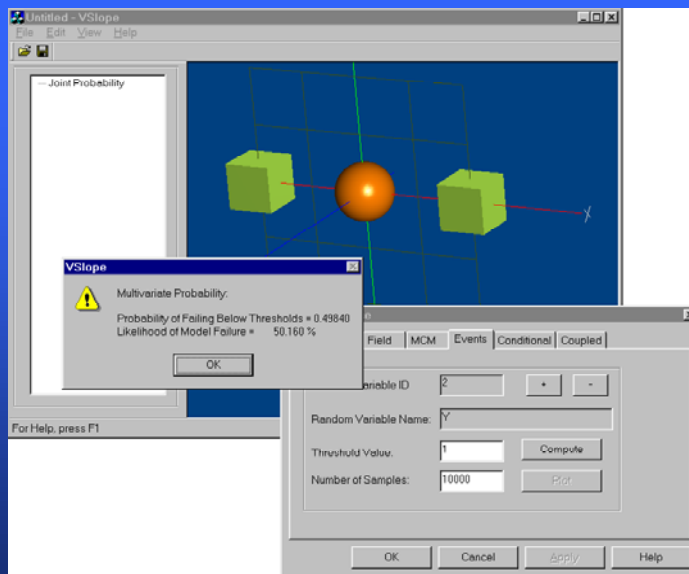
Figure A.1: *PRESAP* Output for Joint Probability Calculations (Screen Capture of Actual Code)
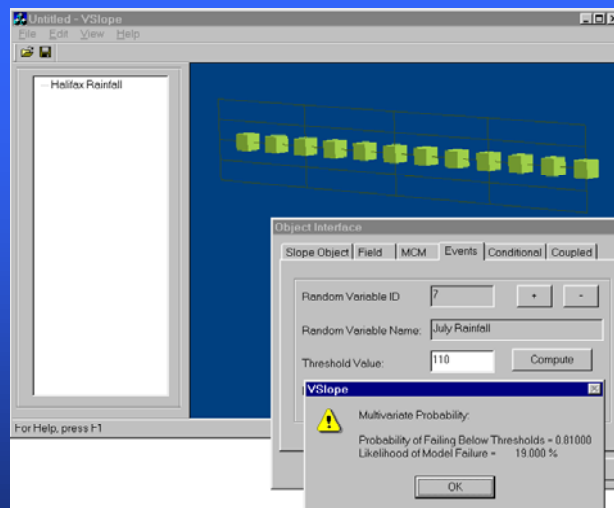

Figure A.2: Joint Probability Calculations for Monthly Rainfall (Screen Capture of Actual Code)
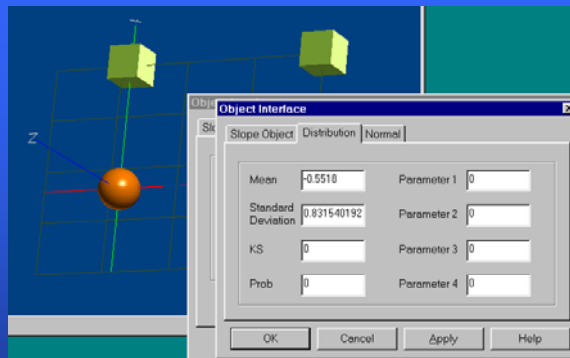
Figure A.3: Conditional Probability Density Function Statistical Parameters (Screen Capture of Actual Code)
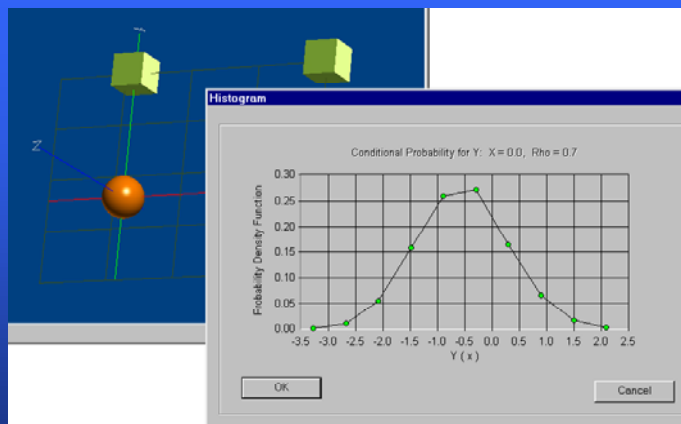

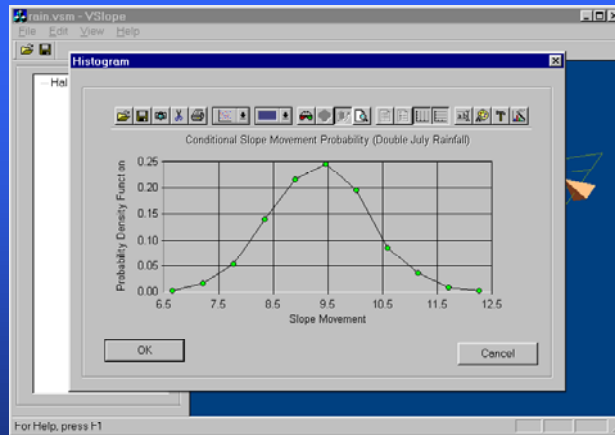Figure A.4: Conditional Probability Density Function (Screen Capture of Actual Code)

Figure A.5: Conditional Probability Density Function for Slope Movement (Computed for Double the Normal Amount of July Rainfall - Screen Capture of Actual Code)